(2)

THE EFFECTS OF DISSOLVED OZONE ON THE CORROSION BEHAVIOR OF 304 STAINLESS STEEL, MONEL 400 AND NAVAL BRASS IN ARTIFICIAL SEA WATER

B.E. Brown and D.J. Duquette
Rensselaer Polytechnic Institute
Materials Engineering Department
Troy, New York 12180-3590

OCTOBER 1993

Final Report to the Office of Naval Research

Contract No. N00014-90-J-1439

The Effects of Dissolved Ozone on the Corrosion Behavior of 304 Stainless Steel, Monel 400 And Naval Brass in Artificial Sea Water

B.E. Brown and D.J. Duquette
Rensselaer Polytechnic Institute
Materials Engineering Department
Troy, New Yerk 12180-3590

CONTENTS

LIST OF TABLES

LIST OF FIGURES

ABSTRACT

The effects of 0.02, 1.2 and 2.3 mg/L ozone on the corrosion behavior of 304 stainless steel, Monel 400, and naval brass were studied at room temperature in artificial sea water at pH 7.5, and the results were compared with those obtained for aerated solutions. Corrosion potentials and cyclic polarization curves were measured after 1 and 17 hour exposure times. Instantaneous corrosion rates were measured using linear polarization resistance (LPR) techniques. Long term (30 day) crevice corrosion experiments were also performed on stainless steel and naval brass in aerated and 0.8 mg/L ozonated solutions.

Increasingly noble corrosion potentials were observed in the cases of stainless steel and Monel with increasing ozone concentration due to the noble redox potential of ozone. Naval brass, on the other hand, maintained a fairly constant corrosion potential, independent of ozone concentration, due to the formation of a bulk corrosion product on the metal surface.

LPR measurements on naval brass reflected the corrosion rates of both zinc and copper due to dezincification occurring on the metal surface. These corrosion rates were found to be independent of ozone concentration and exposure time, although it appears that exposure to 0.02 mg/L ozone after 17 hours resulted in complete dezincification at the surface. The corrosion rate of Monel was found to increase at elevated ozone concentrations, independent of exposure time. Stainless steel, however, showed a decreasing corrosion rate with increasing ozone concentration after one hour due to ozone quickly stabilizing the passive film. Extended exposure caused the corrosion

rate of stainless steel to decrease, independent of ozone concentration, indicating that the presence of either oxygen or ozone fully stabilizes the passive film with time.

Cyclic polarization results for stainless steel showed that increasing ozone concentrations caused the repassivation potential to shift in the active direction relative to the steady state corrosion potential, indicating that pits present on the surface may not repassivate, but continue to grow. Increased ozone concentrations also initially shifted the breakdown potential in the active direction compared to the aerated breakdown potential, indicating a higher susceptibility to crevice corrosion for short exposure times in ozonated solutions.

Increasing ozone concentrations shifted the breakdown and repassivation potentials of Monel 400 active to the steady state corrosion potential, indicating that ozone causes pitting to occur spontaneously in this alloy. Extended exposure caused the repassivation potential to shift noble to the corrosion potential indicating that, although pits may continue to nucleate with time due to the breakdown potential remaining active to the corrosion potential, these pits are likely to repassivate before becoming very large.

Naval brass showed no susceptibility to crevice corrosion when exposed to ozonated or aerated solutions for 30 days. Visual inspection showed there to be only a difference in color of the corrosion product between the aerated and ozonated conditions. In the case of stainless steel, the presence of ozone was found to enhance crevice corrosion. Image analysis showed that the presence of ozone in solution produced slightly more pits with the same median pit area as aerated solutions, but also several very large deep pits.

These results indicate the possibility of a large cathode/small anode effect existing between the highly stabilized passive film formed in the presence of ozone and any inhomogeneity in the metal surface.

1. INTRODUCTION

The strong oxidizing capability of ozone has been utilized as an alternative to chlorination for sterilization of drinking water for over seventy years.[1] Today, as environmental concerns grow about the use of chlorine for industrial oxidizing applications, ozone, with its harmless byproduct of oxygen, is becoming more widely used. Interest has grown from using ozone as a disinfectant in the water treatment industry, into fields such as the pulp and paper industry, which is looking into using ozone as an alternative bleaching agent. There is also great interest in using ozone as a biocide in equipment, such as in heat exchangers and cooling towers, where stagnant water can lead to the proliferation of microbiological corrosion. The corrosion behavior of engineering alloys in ozonated solutions is of particular interest since ozone is a strong oxidizer and rapid corrosion may result. At this time, there exists very little literature on the subject of the corrosion of materials exposed to ozonated solutions and the data which are available are conflicting.

The purpose of this investigation is to evaluate the effects of ozone in artificial sea water on three engineering alloys: 304 stainless steel, Monel 400, and naval brass. These alloys are commonly used in heat exchange systems for naval applications, and represent the spectrum of readily passivating to non-passivating metals.

Ozone concentrations ranging from 0.02 mg/L to 2.3 mg/L were used. The lower end of the range represents typical concentrations for continuous maintenance level biocidal applications. The upper end of the range represents an extreme upset condition.

Electrochemical methods were utilized to measure corrosion rates, as well as breakdown and repassivation potentials of Monel and stainless steel. Testing was performed after 1 and 17 hour exposures in order to analyze whether exposure time affects corrosion behavior. In addition to electrochemical testing, a 30 day crevice corrosion experiment was performed on stainless steel and naval brass. For stainless steel, the crevice corrosion experiments were correlated to electrochemical results.

2. HISTORICAL BACKGROUND

2.1 Ozone Chemistry

Ozone is a strong oxidizer, with a standard electrode potential of 2.07 V (vs. standard hydrogen electrode [SHE]).[2] It is an even stronger oxidizer than chlorine which has a standard electrode potential of only 1.36 V (vs. SHE).[3] Depending upon the pH of the solution in which it is dissolved, molecular ozone will either react directly with components in solution, or decompose into hydroxyl radical, oxygen and hydroxide:[4]

$$2O_3 + H_2O \dashrightarrow OH^{\bullet} + \frac{5}{2} O_2 + OH^-$$

The hydroxyl free radical is a more powerful oxidizer than ozone, with a potential of 2.80 V (vs. SHE).[4] At pH values above 7.5, much of the ozone will decompose into hydroxyl radicals which will react rapidly with water contaminants. Below this pH, molecular ozone is stabilized and only a small fraction of the ozone will be converted into hydroxyl free radicals. Care must be taken when using ozone at elevated pH levels due to the rapid reactions that can occur between the hydroxyl free radicals and water contaminants, with no beneficial effects of disinfection or oxidation occurring.

2.2 Ozone Production

Ozone can be produced using two different methods: ultraviolet (UV) radiation or corona discharge. Ultraviolet radiation uses UV wavelengths of either 254 nm or 186 nm to produce ozone. Using air as a source of molecular

oxygen, these wavelengths produce either 0.01% ozone by weight in air or 0.1%, respectively.[4]

Corona discharge is by far the most popular method of ozone production, but the most inefficient. It utilizes either dry air or oxygen which is subjected to a high voltage between two electrodes. Only about 10% of the energy supplied is used to make ozone, while the remainder is lost as heat.[1] The amount of ozone produced in this system is regulated by the amount of power supplied to the system, as well as the feed gas used. Using air, 1 to 3.5% ozone by weight in air can be produced, while 6 to 12% can be produced using oxygen.[4]

2.3 Ozone Solubility

The solubility of ozone in a solution depends on several factors:

- The concentration of ozone exiting the gas generator
- The temperature of the solution
- The ozone demand in the solution
- The pH of the solution

The theoretical concentration of ozone in solution can be found using the concentration of ozone exiting the generator and Henry's Law: [4]

$$Y=[H][X]$$

Y = Concentration of gas in solution
H = Mole fraction of ozone in gas phase
X = Henry's Law constant

Using Henry's law, ozone has a theoretical solubility of 10 times that of oxygen in pure water, but in solutions other than pure water, it has been

recorded more on the order of 1 to 1.5 times that of oxygen. This discrepancy between theory and practice is due to ozone depleting impurities in real solutions, which are not accounted for in Henry's law, as well as the low partial pressure of ozone.[1,5]

The amount of ozone demanding impurities in the solution affect the decomposition of ozone, with more impurities greatly decreasing the half-life. For pure water, the half-life of ozone is on the order of hours, while in normal water the half life is from 5 to 20 minutes. Impurities which can decrease the half life include soluble iron, magnesia, and bromide, as well as microorganisms.[4]

As was mentioned earlier, ozone will decompose into hydroxyl radicals at pH levels above 7.5. Increasing the pH above this value will cause the half-life of ozone to decrease significantly. At pH 10 the decomposition of ozone is so rapid that no residual ozone can be measured.[4]

2.4 Ozone as a Biocide

Ozone works as a biocide by directly oxidizing the outer shell of microbes. The amount of ozone required to protect a system from microbiological corrosion is relatively small. For systems in which a biofilm layer is already in existence, a constant concentration of 0.2 to 1.0 mg/L ozone is required.[6] In order to maintain protection, after the biofilm has been removed, only 0.02-0.05 mg/L ozone is required.[1,4] These values are well below that considered to be a health hazard by OSHA, of 0.1 ppm by volume in air for 8 hours daily. In order to control biofouling by intermittent exposures to ozone,

concentrations of 0.4 to 0.6 mg/L ozone for 2 hours every other day is sufficient for protection.[4]

2.5 Corrosion of Metals in Ozone

The amount of literature on the corrosion of metals exposed to ozonated solutions is both limited and conflicting. The main source of conflict is that the corrosion data is based on cooling tower water environments utilizing different environmental conditions and few scientific controls.

2.5.1 Iron Based Alloys

For cooling water environments, where temperatures range from 38-49°C, there have been reports of reduced corrosion rates of mild steels when exposed to ozone.[7,8] In a pilot cooling tower, Meier found that the corrosion rates of mild steel decreased from 28 mpy, when chlorine was used alone as a biocide, to 4.6 mpy when ozone alone was used.[8] This decrease in corrosion rate is most likely due to the deposit of scale and corrosion product on the metal surface which was noted in the presence of ozone.

There have also been reports of ozone increasing corrosion rates in cooling water environments.[9-11] Lawson, in an 18 month trial, found that the addition of 0.1 mg/L ozone caused the corrosion rates of mild steel to range from 8-10 mpy, a factor of 4 times higher than corrosion rates reported for a traditional molybdate based water treatment program.[9] Once again, severe fouling and scaling were evident when ozone was used. In laboratory studies using ozone treated cooling water and flow rates of 0.33 m/s,

Strittmatter[10] and Yang[11] found that low ozone concentrations of 0.1 mg/L had no effect on the corrosion rate of mild steel, while the addition of 1 mg/L increased the corrosion rates by a factor of five.

There have also been neutral reports on the effect of ozone on corrosion rates of mild steel in cooling water environments.[10-13] Bird has reported ozone to be neutral in protection of mild steel for open evaporation cooling systems, indicating that conventional corrosion inhibitors, such as sodium nitrate, are more effective.[12] Hettiarachchi, adding 24 ppm Mg^{2+}, 195 ppm Cl^-, 345 ppm SO_4^{2-}, and 88 ppm Cu^{2+} to water to simulate cooling water, found that ozone concentrations of 1.5 to 3 mg/L had no effect on mild steel.[13] In their research, Strittmatter, Yang, and Hettiarachchi have all come to the conclusion that the corrosion rates of mild steel in cooling waters have little dependence on ozone, but are dominated by the water chemistry of the system.[10,11,13]

In deionized and fresh water at 30°C, respectively, both Matsudaira[14] and Kaiga[15] found that ozone levels between 0.2 and 2.1 mg/L increase the corrosion rates of mild steels by a factor of 2-3. The work by Kaiga compared the ratio of the corrosion rates in aerated and 0.3-1.0 mg/L ozonated solutions at different flow velocities. At velocities below 1 m/s, the presence of ozone was found to increase the corrosion rate of mild steel, while the corrosion rate of cast iron was unaffected.[15] At 1 m/s, however, the corrosion rate of mild steel was found to decrease, possibly due to formation of a passive film. Matsudaira's results for mild steel at solution velocities of 0.05-0.1 m/s and a concentration of 2.1 mg/L ozone echoed those of Kaiga, showing an increase in corrosion rate compared to aerated solutions.[14] At a solution velocity of

1.7 m/s, however, ozone had no effect on the corrosion rate of mild steel compared to aerated solutions. In contrast to these studies, Walton found the corrosion rate of mild steel to decrease when exposed to 2 mg/L of ozone.[16]

As with mild steel, there are varying reports with regard to the effect of ozone on the corrosion of stainless steels. In cooling water environments, Meier[8] has reported that ozone has no significant effect on the corrosion of stainless steel, while Kaiga[15] reports a significant increase in corrosion rate in stainless steel when exposed to 0.8 mg/L ozone. In deionized water, Matsudaira found there to be no effect of ozone or flow rate on the corrosion rates of 303, 403, and 430 stainless steels.[14] In chloride solutions, Lu[17] and Brown[18] have shown that the presence of ozone affects the crevice corrosion susceptibility of 304 and 304L stainless steels, shifting the breakdown and corrosion potentials more noble and the repassivation potential more active. These changes indicate that ozone increases the susceptibility to pitting and crevice corrosion.

2.5.2 Copper Alloys

In cooling tower environments, the corrosion rates of copper and brass were found to be reduced by the presence of ozone at levels of 0.05 mg/L.[7,19,20] This effect was attributed to a thin protective layer forming on the metal surface. In synthetic cooling water, Strittmatter[10] and Yang[11] found there to be little effect of 0.1 mg/L ozone upon the corrosion rates of copper, 90 Cu-10Ni, admiralty brass, and 70Cu-30Ni; however these corrosion rates increased by a factor of 5 to 10 when the concentration was increased to

1 mg/L ozone. In contrast, Hettiarachchi found there to be no effect of 1.5 to 3 mg/L ozone on copper in synthetic cooling water.[13]

In deionized water environments, the corrosion rates of copper and brass were found to increase by a factor of 5 to 6 with the addition of 2 mg/L ozone, regardless of flow rate.[14] In fresh water, Kaiga similarly found that ozone concentrations of 0.5-0.9 and 3.2-3.5 mg/L increased the corrosion rate of copper by a factor of 5 at a velocity of 1 m/s.[15] This study also showed, however, that a lower flow rate of 0.53 m/s decreased the corrosion rate of copper by a factor of 2 at an ozone concentration of 1.2 mg/L.[15] In stagnant solutions containing 0.5N of NaCl, Lu found the corrosion rate of 70Cu-30Ni to decrease in the presence of 2.0 mg/L ozone.[17]

2.5.3 Other Alloys

Only a few alloys, other than those mentioned above, have been studied in ozonated aqueous solutions. For instance, Walton found that the corrosion rate of aluminum was decreased in the presence of 2 mg/L ozone.[16] Also, it has also been found that the corrosion rates of titanium and Cr-Ni alloys are unaffected by the presence of ozone, due to the formation of a thin protective layer.[19,20]

3. EXPERIMENTAL PROCEDURE

3.1 Specimen Preparation

Samples of 304 stainless steel, Monel 400 and naval brass were used in this study. The elemental content of each of these alloys, given by the supplier, is listed in Tables I-III.

Table I. Composition of 304 Stainless Steel

Element	C	Mn	P	S	Si	Cr	Ni	Mo	Cu	Co	N	Fe
Weight Percent	0.05	1.7	0.03	0.02	0.05	18.4	8.1	0.19	0.03	0.07	0.05	71.3

Table II. Composition of Monel 400

Element	C	Mn	P	S	Si	Cr	Ni	Fe	Al
Weight Percent	0.10	1.0	-	0.02	0.08	32.2	64.7	1.88	0.04

Table III. Composition of Naval Brass

Element	Cu	Fe	Pb	Sn	Zn
Weight Percent	59-62	0.15 max	0.2 max	0.5-1.0	Rem.

Stainless steel in the form of wire, 0.04 cm in diameter, was utilized since it was found that sheet samples of this material mounted in epoxy formed crevices between the sample and mount material which had a large

effect on the electrochemical results. The wire was shaped into a hook which was partially submerged, to only expose the circumference of the wire. Samples of Monel 400 sheet (1 cm^2) were mounted in epoxy (no crevice effect was noted for these samples). Naval brass samples were cylindrical in shape, 1.86 cm in diameter and 1.27 cm high, and were fixtured as shown in Figure 3.1. All samples were ground to 600 grit SiC, then rinsed in distilled water.

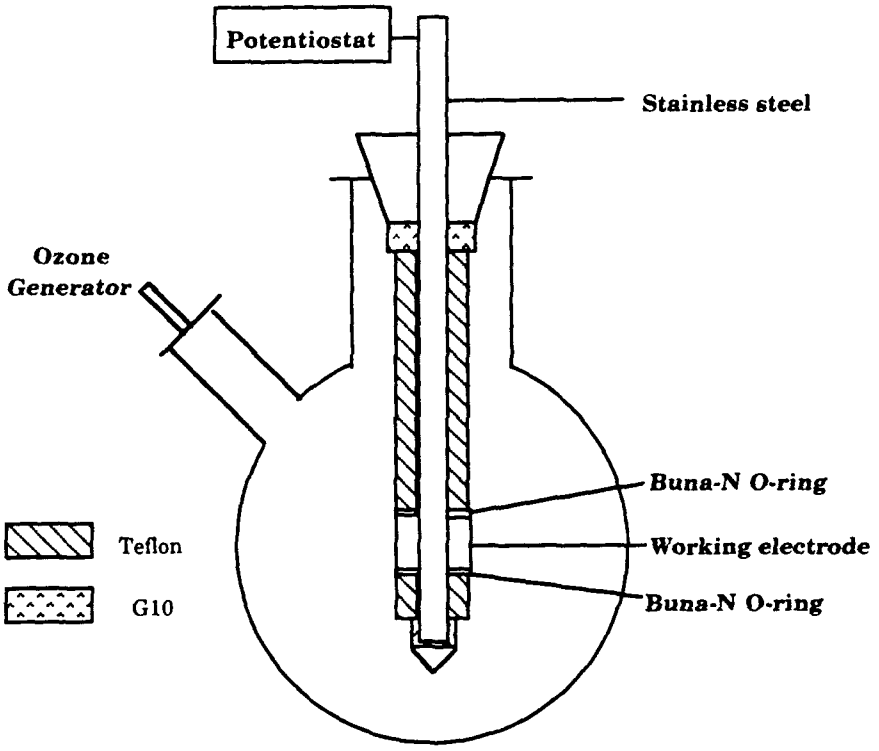

Figure 3.1 Cell set-up used for testing naval brass.

3.2 Solutions

Solutions of artificial sea water were continuously ozonated during experimentation with a corona discharge ozone generator using air as the car-

rier gas. Ozone concentrations were measured using the standard Diethyl-P-Phenylenediamine (DPD) method prior to experimentation.[21] The pH of the solutions was maintained at a level of 7.5. Experiments were performed at 25°C for conditions of 0.02, 1.2 and 2.3 mg/L of ozone, as well as in aerated solutions. Solutions were renewed after each test.

3.3 Electrochemical Test Procedures

A typical electrochemical set-up was used to obtain data (Figure 3.2). After immersion in solution, samples of Monel and stainless steel were cathodically polarized at -1.0 V vs. SCE for five minutes in order to remove any prior surface film. The steady state corrosion potential was measured after either 1 hour, for short term exposure, or 17 hours for long term exposure. Linear polarization resistance and cyclic polarization curves were then measured. Separate samples were used to obtain 1 hour and 17 hour results.

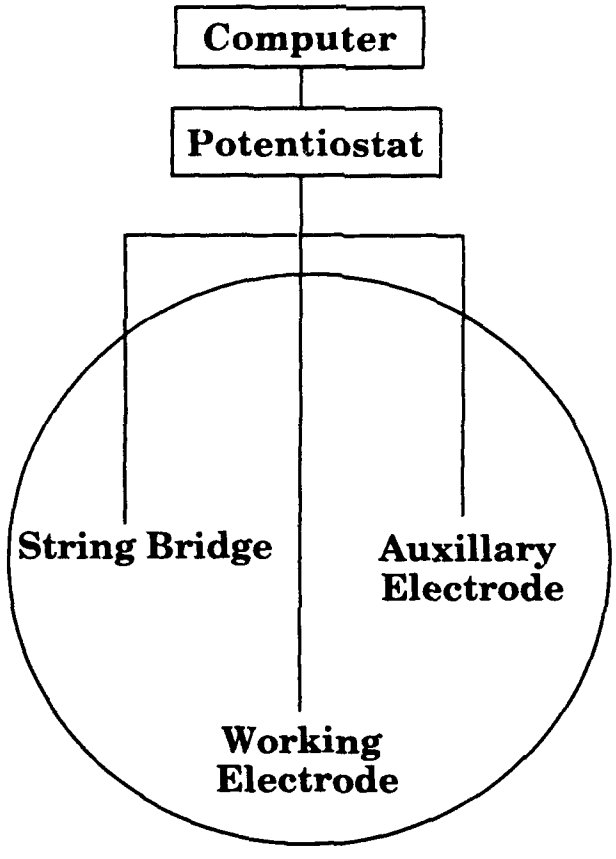

Figure 3.2 Typical electrochemical set-up.

3.3.1 Linear Polarization Resistance

Linear polarization resistance (LPR) was used to rapidly obtain corrosion rate data from a simple polarization scan. A potentiostat was utilized to polarize the material to approximately 10 mV in the noble direction relative to the corrosion potential of the metal using a scan rate of 0.3 mV/s. The slope of the resulting potential versus current plot is called the polarization resistance, R_p, which has the dimensions of ohms. This value was used to

calculate corrosion rates based on the theory that the surface of the metal is a simple resistor. The equation utilized is the Stern-Geary equation:[22]

$$i_{CORR} = \frac{\beta_a \beta_c}{2.303 (\beta_a + \beta_c)} \left(\frac{1}{R_p} \right)$$

where β_a and β_c are the anodic and cathodic Tafel slopes, respectively. Care must be taken in comparing corrosion rates based on LPR results from two different studies, as the assumptions made about the values of the anodic and cathodic Tafel slopes may vary and cause differences up to a factor of 4.8 (see Appendix).

3.3.2 Crevice Corrosion Testing

Although generalized corrosion is a very important measurement to obtain on materials in corrosive environments, it is also important to evaluate the effects of the environment on localized corrosion. One method to determine susceptibility to crevice corrosion is to form a crevice on the material, then immerse it in the environment of interest. A fixture called a crenelated washer is normally used to simulate multiple crevices which might be seen in an industrial application. This washer is made of a chemically inert material which has grooves cut into it (Figure 3.3). Creviced washers, such as this, were affixed to polished samples of naval brass and stainless steel prior to immersion in aerated and 0.8 mg/L ozonated artificial sea water solutions. Three samples were tested for each condition for a period of 30 days.

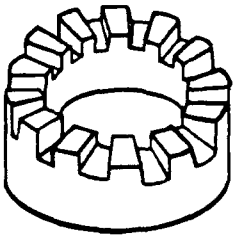

Figure 3.3 Crenelated Washer

Image analysis was performed on the stainless steel crevice corrosion samples by digitizing video images of the sample surface at a magnification of 50x. The software used for the analysis was NIH Image 1.47 which is a public domain image processing and analysis program for the Macintosh™. Depth measurements of the pits were taken using a diamond stylus profilometer and were compared to metallographic cross sections.

3.3.3 Cyclic Polarization

To rapidly assess the localized corrosion behavior of stainless steel and Monel, an electrochemical technique called cyclic polarization was used. The material was polarized into the transpassive region and then the scan was reversed. For Monel, the cyclic polarization curves were started at the steady state corrosion potential and then polarized anodically at 10 mV/s to a potential of +300 mV vs. SCE, where the scan was reversed. Using a scan rate of 1.3 mV/s, stainless steel scans were started at -1.0 V vs. SCE and were polarized anodically to a current of 3 mA before reversing. Figure 3.4 shows a typ-

ical cyclic polarization diagram for 304 stainless steel in aerated artificial sea water obtained in this study.

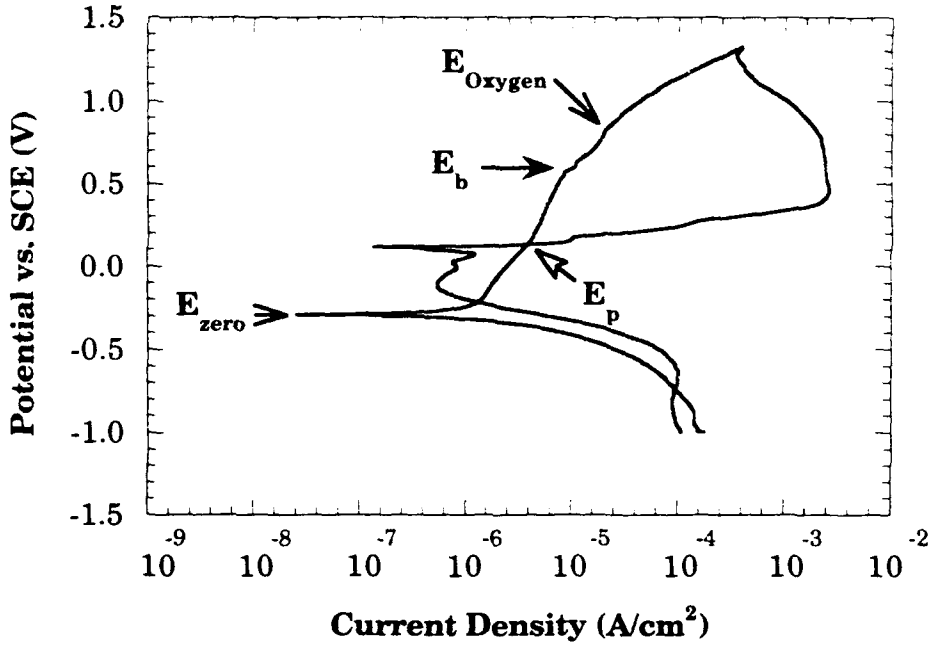

Figure 3.4 Cyclic polarization curve of 304 stainless steel after 1 hour of exposure in aerated artificial sea water at 23°C, pH 7.5.

From the diagram, the breakdown potential, E_b, the repassivation potential, E_p, and the zero current corrosion potential, E_{zero}, can be obtained as shown. The breakdown potential is the potential at which the passive film breaks down, while the repassivation potential is the potential below which existing pits cease growing, nor will any new pits form. The reversible potential of oxygen, E_{oxygen}, is also shown in this diagram and corresponds to another change in slope of the polarization curve. At this potential, the production of oxygen from water occurs and causes an increase in the corrosion rate

of the metal. The value of E_{oxygen} taken from the cyclic polarization curve shown here corresponds closely to that calculated in the Appendix from the Nernst equation for an aerated solution.

Another aspect of the cyclic polarization diagram is the hysteresis loop which forms when the potential scan is reversed on a passivating metal which is susceptible to pitting and crevice corrosion. This phenomenon is indicative of the growth and formation of pits on the surface of the metal, with the area of the hysteresis loop corresponding to the amount of energy that has gone into the formation and growth of pits. Although this area can be measured, there are a number of factors influencing it which cannot be controlled, i.e., the number of pit initiation sites and the uniformity of pit growth. It is best used as only an indicator as to whether a passive material is susceptible to pitting or crevice corrosion in a given environment.

Depending upon the scan rate used to obtain cyclic polarization curves, the values reported from such testing can be affected. If the metal is scanned too fast, the reactions occurring at the surface may not have had sufficient time to come to a steady state, affecting the resultant polarization curve. An excessively rapid scan rate can also cause a material to appear not susceptible to crevice corrosion by showing no apparent hysteresis loop, when in fact there is only a very slight one because the material has only had time to initiate and grow a few pits. This was the case for stainless steel, where a slower scan rate of 1.3 mV/s was used, as the faster scan rate of 10 mV/s failed to produce pitting and the formation of a hysteresis loop.

4. RESULTS & DISCUSSION

4.1 Steady State Corrosion Potential

4.1.1 304 Stainless Steel

Figure 4.1 shows that, as the ozone concentration was increased, the corrosion potential of stainless steel became increasingly noble, reaching a plateau at 200 mV noble to the aerated condition at ozone concentrations of 1.2 and 2.3 mg/L. After 17 hours of exposure all values shifted in the noble direction compared to those of 1 hour.

The noble increase in corrosion potential of stainless steel with increasing ozone concentration is due to the mixed potential being controlled by the cathodic reduction of ozone:

$$O_3 + 2H^+ + 2e^- \rightarrow O_2 + H_2O$$

Ozone has a noble redox potential of 2.07 V vs. SHE, therefore, when ozone is present in sufficient concentrations, a noble shift in potential is observed. The noble shift in potential for all conditions after 17 hours indicates stabilization of the passive film of the stainless steel with time, with increasing ozone concentrations having a more significant stabilization effect than the presence of oxygen alone (aerated condition).

4.1.2 Monel 400

It was found that the steady state corrosion potential of Monel 400 became increasingly noble with increasing ozone concentration, shifting a total of 200 mV in the noble direction relative to the aerated condition when 2.3 mg/L of ozone was present (Figure 4.2). Extended exposure caused only a slight noble increase in corrosion potential for all conditions.

As with stainless steel, the increase in the corrosion potential of Monel 400 with increasing ozone concentration is due to the noble redox potential of ozone. This is confirmed by the 200 mV shifted which is noted for both alloys at elevated ozone concentrations. In the case of Monel however, prolonged exposure indicates that the passive film is only slightly stabilized with time.

4.1.3 Naval Brass

Figure 4.3 shows that the presence of ozone had no effect on the corrosion potential of naval brass after one hour of exposure. After 17 hours of exposure, all conditions, with the exception of 2.3 mg/L ozone, showed a slight noble shift in potential of 20 to 30 mV. A color change was also noted on the surface of the metal, with a brown tarnish forming under aerated and low ozone conditions and gold colored corrosion product forming at elevated ozone concentrations.

The lack of response in the steady state corrosion potential of naval brass to increasing ozone concentration after one hour indicates that a diffusion barrier of corrosion product exists at the surface of the naval brass. This corrosion product is most likely a surface oxide, of either Cu_2O, CuO, or a

combination of both, through which Cu^{++} must diffuse in order to cause a shift in the potential.

With increased exposure time, the composition of this surface layer changes, as indicated by the difference in color of corrosion product. Naval brass in aerated and low ozone conditions appears to undergo dezincification. This process can occur by one of two mechanisms. One mechanism involves the diffusion of zinc to the surface of the alloy where it undergoes preferential corrosion, leaving a copper rich residue.[23] The other mechanism involves the corrosion of the alloy and redepositing of copper as a porous layer.[23] Dezincification is usually retarded in this alloy due to the addition of 1% Sn, however, stagnant solutions, as well as inorganic scale formation can cause an increase susceptibility to this process.[23] Preferential corrosion of zinc or plating of copper at the surface could explain the slight noble shift in potential of naval brass exposed to aerated and low ozone concentrations, as the standard redox potential of copper is 0.337 V and the standard redox potential of zinc is 0.763 V.

The lack of a noble shift in the steady state corrosion potential of naval brass when exposed to 2.3 mg/L ozone for 17 hours indicates that ozone, either by itself or by the oxygen created by its breakdown, has stabilized the oxide which is present after one hour, preventing or retarding the process of dezincification.

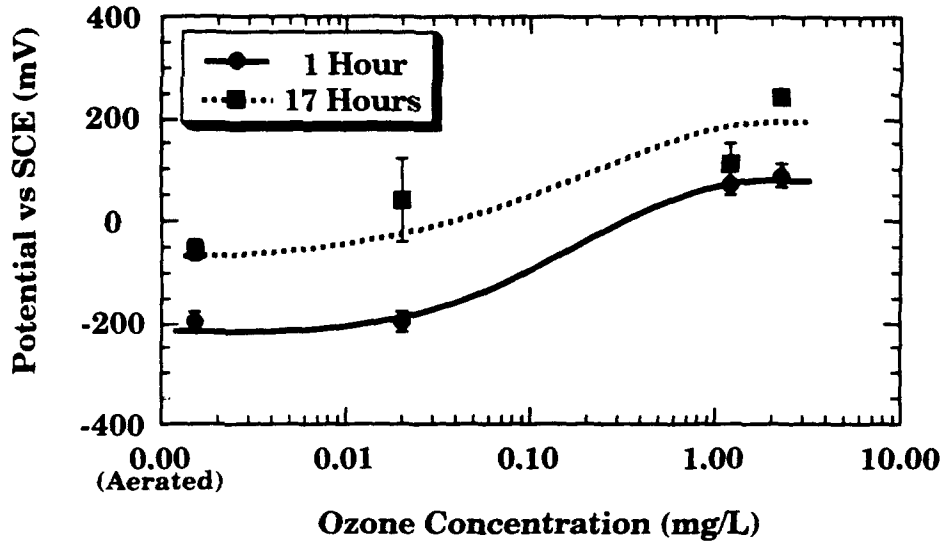

Figure 4.1 Steady state corrosion potential of 304 stainless steel as a function of ozone concentration in artificial sea water at 23°C, pH 7.5.

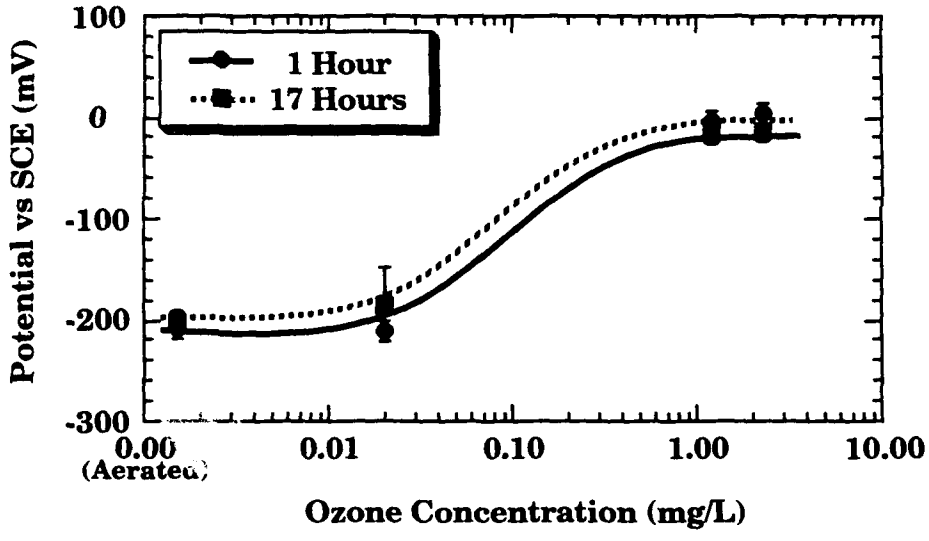

Figure 4.2 Steady state corrosion potential of Monel 400 as a function of ozone concentration in artificial sea water at 23°C, pH 7.5.

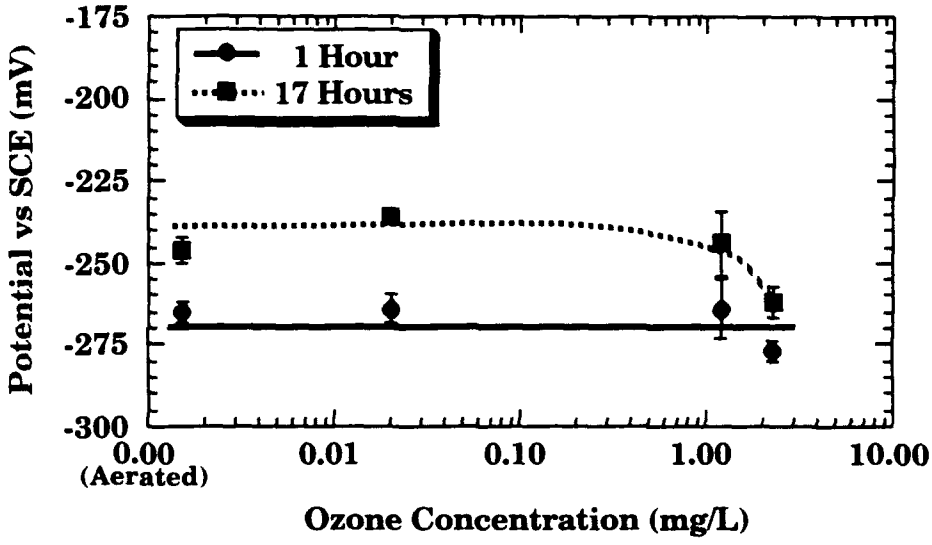

Figure 4.3 Steady state corrosion potential of naval brass as a function of ozone concentration in artificial sea water at 23°C, pH 7.5.

4.2 Breakdown Potential

4.2.1 304 Stainless Steel

It was found that there was little difference between the breakdown potentials of stainless steel for either aerated or 0.02 mg/L ozone conditions at 1 and 17 hour exposure times (Figure 4.4). At increased ozone concentrations and 1 hour of exposure, the breakdown potential was shifted 100 mV in the active direction relative to the aerated and 0.02 mg/L ozone conditions. After 17 hours of exposure however, this trend was reversed and the break-

down potential for elevated ozone concentrations was shifted 200 mV in the noble direction relative to the aerated and 0.02 mg/L conditions.

In general, crevice corrosion susceptibility increases as the breakdown potential shifts active and comes closer to the steady state corrosion potential. If the corrosion potential is at or near the breakdown potential, the material will actively pit. Although the breakdown potential is at least 400 mV noble to the steady state corrosion potential in all cases, these results indicate that short term exposure to elevated ozone concentrations increases the susceptibility of 304 stainless steel to pitting and crevice corrosion due to the active shift in the breakdown potential relative to the aerated and low ozone conditions.

This result seems to contradict the hypothesis that increased ozone concentrations produce a highly stabilized passive film. However, this deviation can be explained if, after an hour, there are ruptures or defects present in the passive film. Ruptures in the passive film would produce a patchwork of less stabilized regions within the highly stabilized film. These less stabilized regions would become small anodes surrounded by a large, more passive cathodic film, producing a galvanic effect which could account for an increase in crevice corrosion susceptibility. A significant number of defects in the passive film would also increase the crevice corrosion susceptibility, as they would create a path by which metal ions could migrate to the surface and undergo reaction. Extended exposure to elevated ozone concentrations provides sufficient time for the development of a thicker passive film. This thicker passive film would be likely to have fewer ruptures, as well as a longer diffusion path for any metal ions which might travel through defects in the pas-

sive film, resulting in a decrease in crevice corrosion susceptibility. Further, this decrease in susceptibility with extended exposure, relative to the aerated condition, is a definite indicator that the passive film formed in the presence of ozone is more stable than that produced by oxygen alone. This conclusion is also supported by the noble increase in the steady state corrosion potential at elevated ozone concentrations discussed earlier.

4.2.2 Monel 400

No difference was found between the breakdown potential of Monel 400 under aerated and low ozone conditions. With extended exposure, these values were found to shift slightly noble, causing a slight decrease in crevice corrosion susceptibility with time, indicative of a time-enhanced passive film.

At elevated ozone concentrations however, no breakdown potential was observed, independent of exposure time (Figure 4.5). At these ozone levels, the corrosion potential shifted noble to the breakdown potential and no passive region was evident. These results indicate that the material will actively pit in solutions exposed to increased ozone concentrations. One can conclude from these results that elevated ozone concentrations increase the crevice corrosion susceptibility of Monel 400.

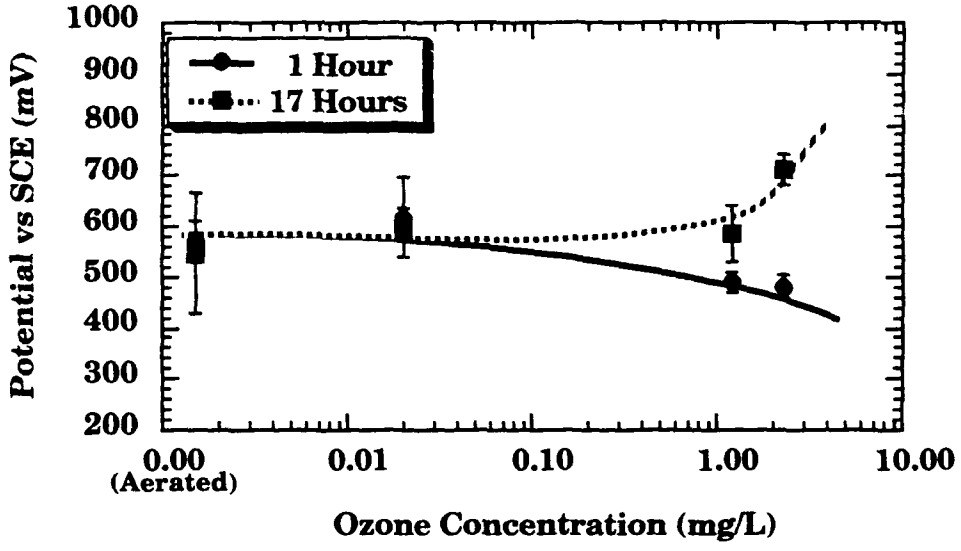

Figure 4.4 Breakdown potential of 304 stainless steel as a function of ozone concentration in artificial sea water at 23°C, pH 7.5.

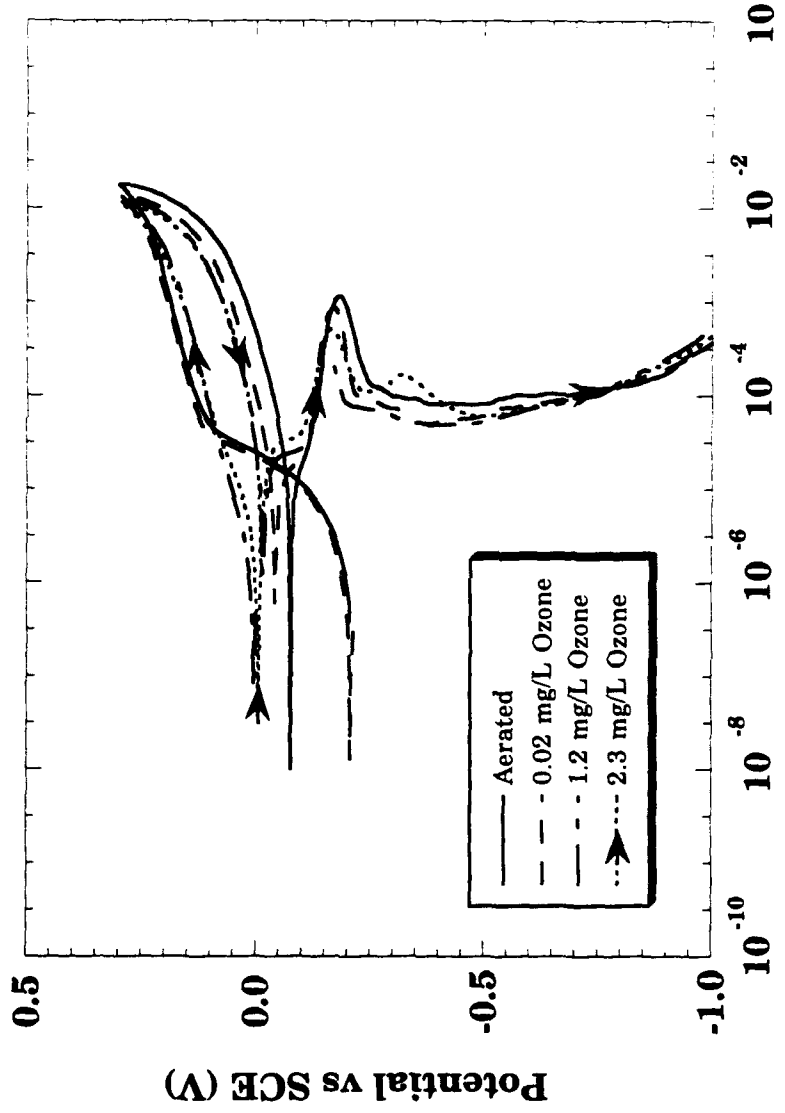

Figure 4.5 Cyclic polarization curves of Monel 400 as a function of ozone concentration after 1 hour of exposure in artificial sea water at 23°C, pH 7.5.

4.3 Repassivation Potential

4.3.1 304 Stainless Steel

Figure 4.6 shows that the presence of ozone has no significant effect on the repassivation potential of 304 stainless steel after 1 and 17 hour exposure times. The difference between the repassivation and steady state corrosion potential (Figure 4.7) shows that the steady state corrosion potential becomes equal or noble to the repassivation potential at elevated ozone concentrations for both 1 and 17 hour exposure times.

The repassivation potential is the potential below which pits on the surface may repassivate and stop growing depending on the depth of the pit and the current driving pit corrosion. The difference between the repassivation and steady state corrosion potential is an indicator of a material's ability to repassivate surface pits during exposure to a solution. When this difference is small, or negligible, it is unlikely that the repassivation of pits or crevices will occur. These results indicate that increased ozone concentrations will cause any crevices or pits present on the surface of stainless steel to grow since the steady state corrosion potential is noble to the repassivation potential.

4.3.2 Monel 400

The repassivation potential of Monel was shifted 40 mV in the noble direction by the presence of ozone (Figure 4.8). Extended exposure caused all

conditions to shift further in the noble direction, maintaining the same trend as at 1 hour of exposure. As in the case of stainless steel, the difference between the repassivation and steady state corrosion potential of Monel 400 drops to zero at elevated ozone concentrations after 1 hour of exposure (Figure 4.9). After 17 hours, the difference becomes slightly higher for elevated ozone concentrations as the repassivation potential shifts noble to the steady state corrosion potential.

Recalling that the breakdown potential was found to be active to the steady state corrosion potential at elevated ozone concentrations, these results indicate that Monel will undergo active pitting and continued pit growth after an hour of exposure. As exposure time is increased, pits will continue to form, but the shift in the repassivation noble to the steady state corrosion potential indicates that pits or crevices on the surface will begin to repassivate and stop growing.

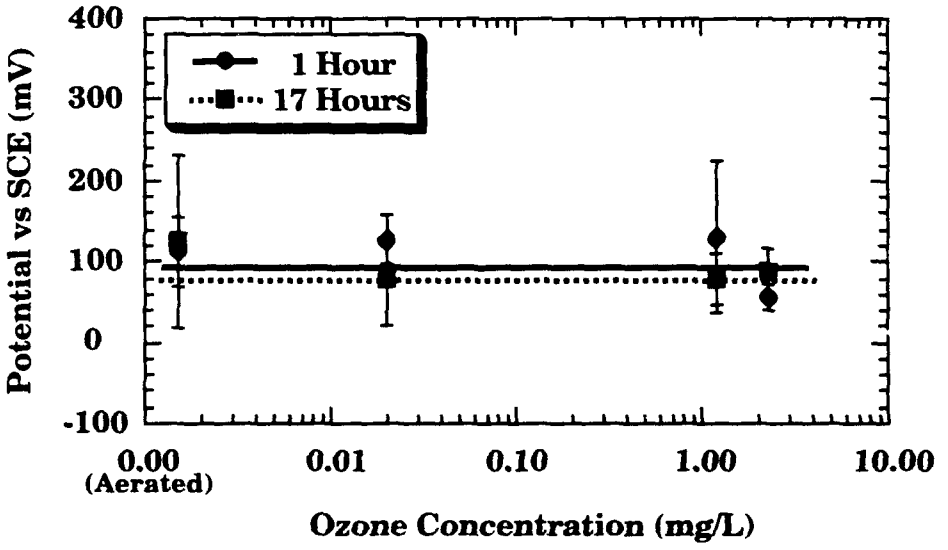

Figure 4.6 The repassivation potential of 304 stainless steel as a function of ozone concentration in artificial sea water at 23°C, pH 7.5.

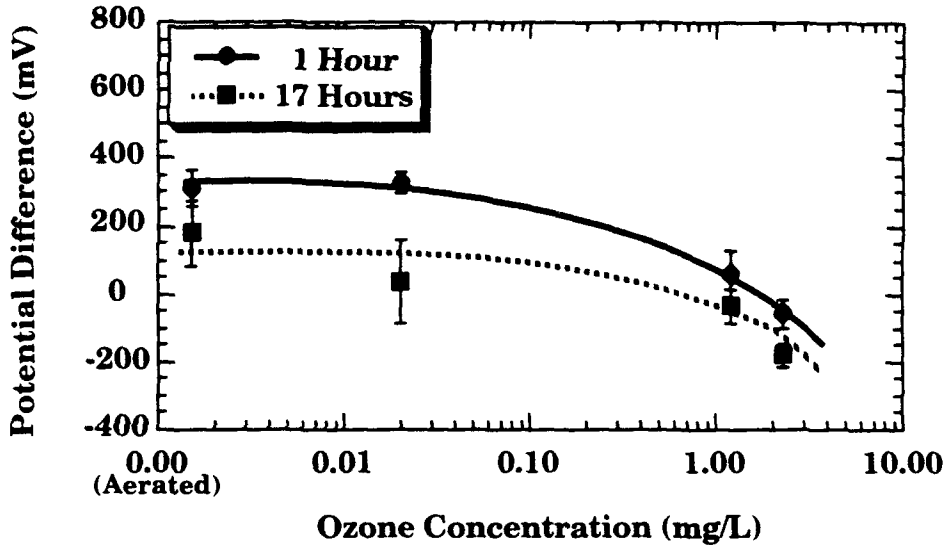

Figure 4.7 The potential difference between the repassivation and steady state corrosion potential of 304 stainless steel as a function of ozone concentration in artificial sea water at 23°C, pH 7.5.

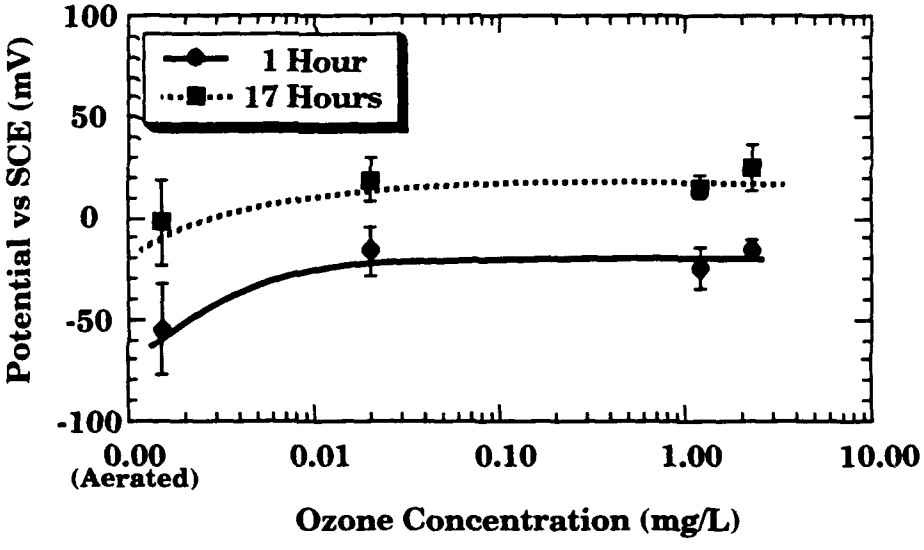

Figure 4.8 The repassivation potential of Monel 400 as a function of ozone concentration in artificial sea water at 23°C, pH 7.5.

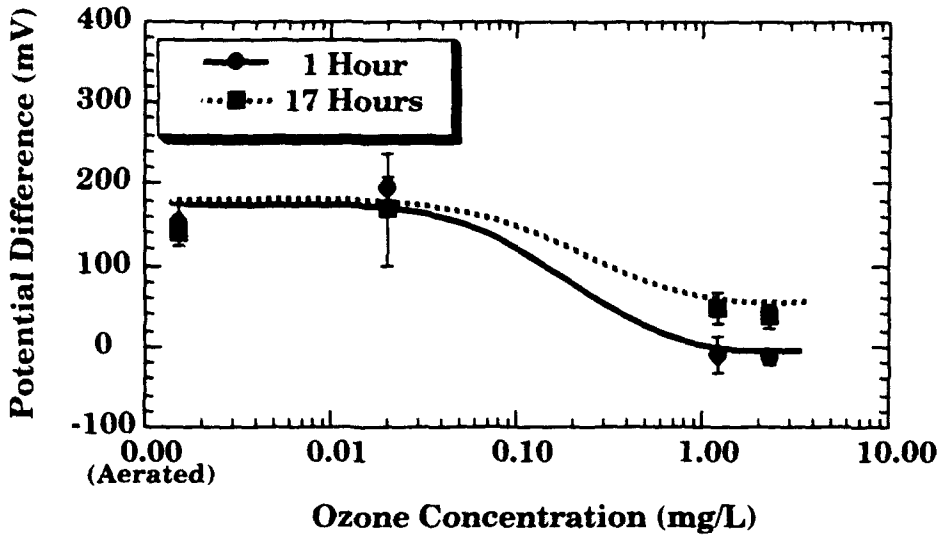

Figure 4.9 The potential difference between the repassivation and the steady state corrosion potential of Monel 400 as a function of ozone concentration in artificial sea water at 23°C, pH 7.5.

4.4 Crevice Corrosion Testing

Visual inspection of the 30 day crevice corrosion samples of 304 stainless steel showed that samples exposed to 0.8 mg/L ozone produced a few very large deep pits compared to the aerated condition (Figures 4.10 and 4.11). Image analysis at 50x showed that there were slightly more pits when the samples were exposed to ozone. The average pit area was larger in the ozonated case, however, the median value of the pit area is less than that of the aerated condition, indicating that there were only a few extremely large pits on the samples exposed to ozone. Several measurements of pit depth were taken on the largest pits for each condition using a profilometer. These values were found to range from 0.002 to 0.06 mm for the ozonated condition

and 0.005 to 0.04 mm for the aerated condition. Metallographic analysis showed that larger pits were much deeper than observed using profilometry techniques.

It was expected that stainless steel samples exposed to ozone would develop larger and more numerous pits than the aerated condition, due to both the active shift in the breakdown potential in highly ozonated solutions after 1 hour, and the steady state corrosion potential being equivalent to the repassivation potential. The presence of very large pits on the ozonated samples suggests that a large number of pits formed initially and continued to grow, coalescing into one large pit. It was expected that pits would be larger in the case of samples exposed to ozone due to the repassivation potential being equivalent to the steady state corrosion potential under ozonated conditions. Because of this, any pit or crevice present on the surface would undergo active corrosion and would not be likely to repassivate. The driving force for the enlargement of the pits may be due to the continued stabilization of the passive film by ozone with time which could have caused a small anode (pit) – large cathode (passive film) effect.

Although a 30-day crevice corrosion test was not performed on Monel 400, the electrochemical results indicate that this material would be very susceptible to pitting and crevice corrosion. Future work in this area will include crevice corrosion testing of this material to confirm electrochemical results.

It was found that samples of naval brass showed no evidence of crevice corrosion in either aerated or 0.8 mg/L ozone solutions. However, differences in the colors of corrosion product were noted visually. Samples exposed to

ozone developed a gold colored corrosion product, while aerated solutions developed a whitish-green corrosion product, indicative of copper.

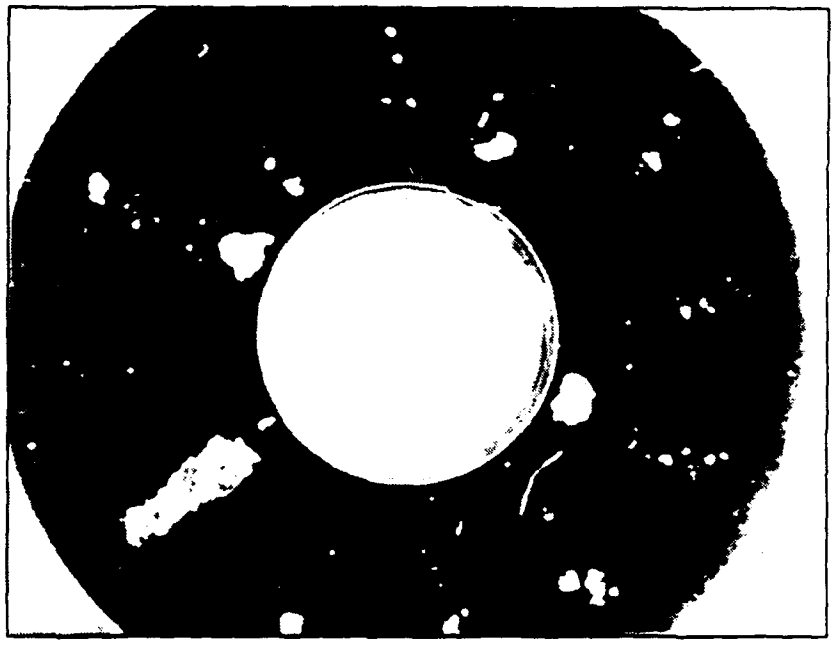

Figure 4.10 30 day crevice corrosion test of 304 stainless steel exposed to 0.8 mg/L of ozone in artificial sea water at 23°C, pH 7.5. 6x.

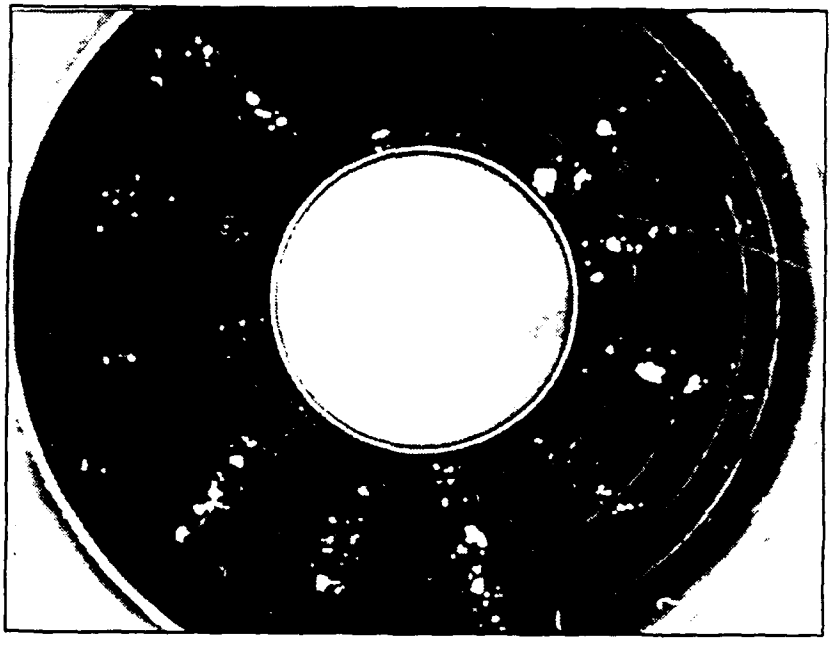

Figure 4.11 30 day crevice corrosion test of 304 stainless steel exposed to aerated artificial sea water at 23°C, pH 7.5. 6x.

4.5 Corrosion Rate Measurements

The Tafel slopes, β_a and β_c, were assumed to equal 0.12 in order to calculate the corrosion rates of each material from the slopes obtained from the LPR tests. These values of Tafel slope were used because the values of corrosion rate they produce should vary no more than 2x the actual corrosion rate. See Appendix for equations used in calculations.

4.5.1 304 Stainless Steel

The corrosion rate of stainless steel was shown to decrease at elevated ozone concentrations, producing a corrosion rate which was half that of the aerated condition (Figure 4.12). With extended exposure, a decrease in corrosion rate occurred for all conditions, with the presence of ozone having no effect on corrosion rate.

These results show that elevated ozone concentrations initially stabilize the passive film faster than oxygen (aerated condition). However, as time progresses the passive film formed by oxygen in aerated solutions equals the stability of that produced by ozone, yielding similar corrosion rates. There are several literature sources which have also shown ozone to have no effect on the corrosion rate of stainless steel.[8,14] In these cases, however, corrosion rates for short exposure times were not measured.

4.5.2 Monel 400

Monel showed increasing corrosion rates with increasing ozone concentrations, independent of exposure time (Figure 4.13). The corrosion rate for

2.3 mg/L ozone was found to be three times higher than for the aerated condition.

This result, in conjunction with results which indicate increased crevice corrosion susceptibility, shows that elevated ozone concentrations are extremely detrimental to this alloy.

4.5.3 Naval Brass

Linear polarization resistance measurements of naval brass showed two separate slopes when the potential was shifted in the active direction relative to the corrosion potential, indicating two distinct corrosion events. These are believed to correspond to the corrosion rates of zinc and copper, respectively, due to dezincification in stagnant sea water (Figure 4.14).

Large corrosion rates were observed when the sample was initially polarized, and are believed to reflect the corrosion rate of zinc. These were found to be independent of ozone concentration after one hour of exposure (Figure 4.15). Extended exposure caused the corrosion rates to decrease slightly for all conditions, with the exception of 0.02 mg/L, where a large decrease in corrosion rate was noted. The second slope, believed to reflect the corrosion rate of copper, produced much lower corrosion rates which were independent of ozone concentration and exposure time (Figure 4.16).

Uhlig reports that the corrosion rate of copper in sea water is approximately 0.03 mm/y, while that of zinc and naval brass range from 0.02-0.1 mm/y.[23,24] It is likely that the initial slope measured in the LPR scan represents the corrosion rate of zinc in sea water, as this component of naval brass appears to control the corrosion rate of the alloy, as seen by the similar

corrosion rates for zinc and naval brass in sea water. The results reported here are somewhat higher than those reported by Uhlig for the corrosion rates of zinc in sea water. This can be attributed to dezincification being more rapid for our experiment due to a combination of enhanced dezincification by polarization, as well as the fact that most dezincification occurs upon initial exposure and the results given by Uhlig were for weight loss measurements after several years. The anomalous result in Figure 4.15 for the condition of 0.02 mg/L ozone after 17 hours of exposure correlates with the measured corrosion rate of copper, indicating that this condition caused complete dezincification at the surface.

Elevated ozone concentrations appear to have no significant effects on the corrosion behavior of naval brass compared to the aerated condition. A difference was expected to be seen after extended exposure due to the difference in the appearance of the corrosion product between the two conditions. It is possible that the oxide which forms on the surface of samples exposed to the highly ozonated solution becomes unstable when polarized, leading to results similar to the aerated condition.

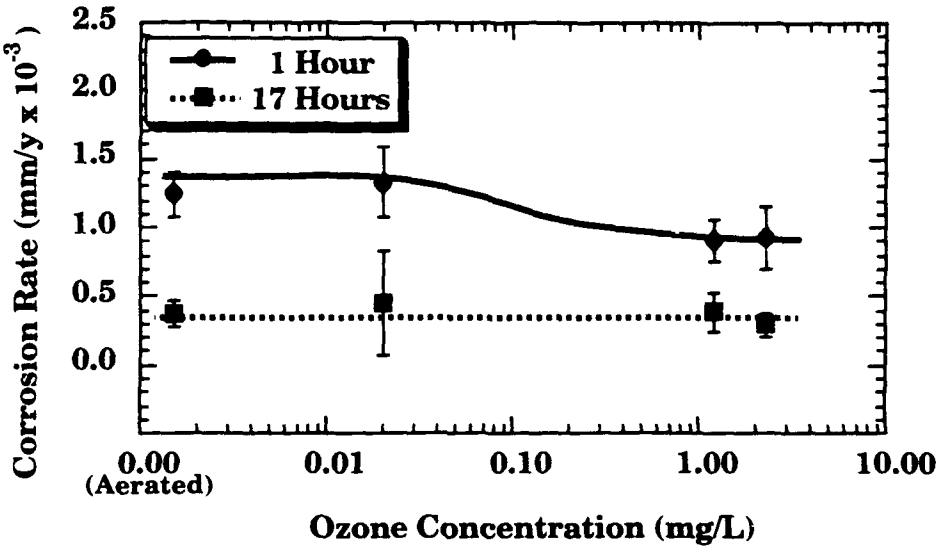

Figure 4.12 The corrosion rate of 304 stainless steel as a function of ozone concentration in artificial sea water at 23°C, pH 7.5.

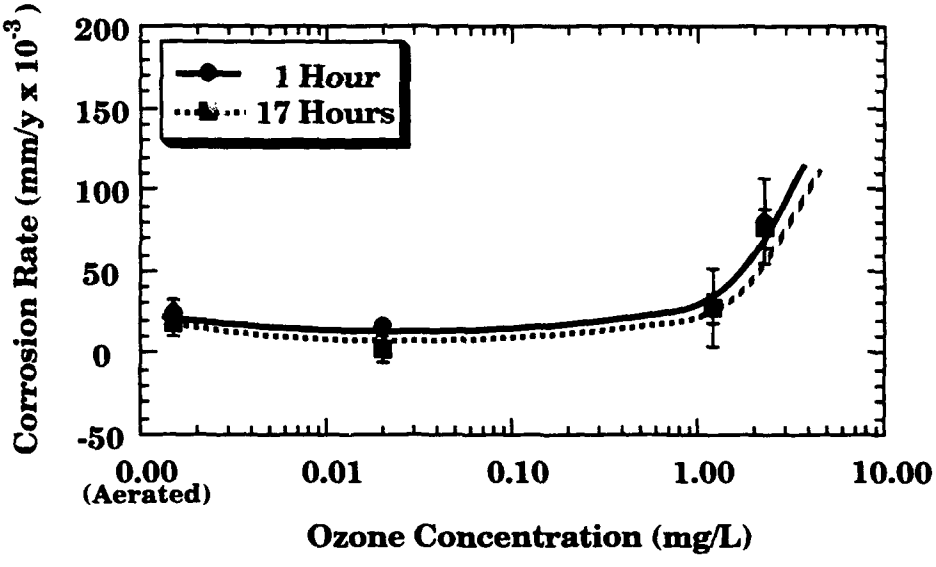

Figure 4.13 The corrosion rate of Monel 400 as a function of ozone concentration in artificial sea water at 23°C, pH 7.5.

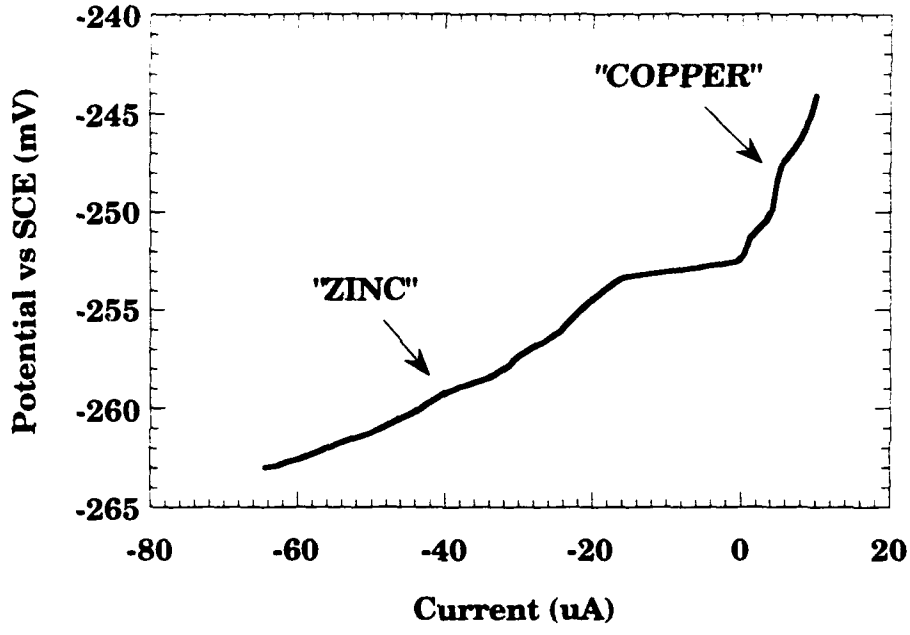

Figure 4.14 Linear polarization diagram of naval brass in aerated artificial sea water at 23°C, pH 7.5.

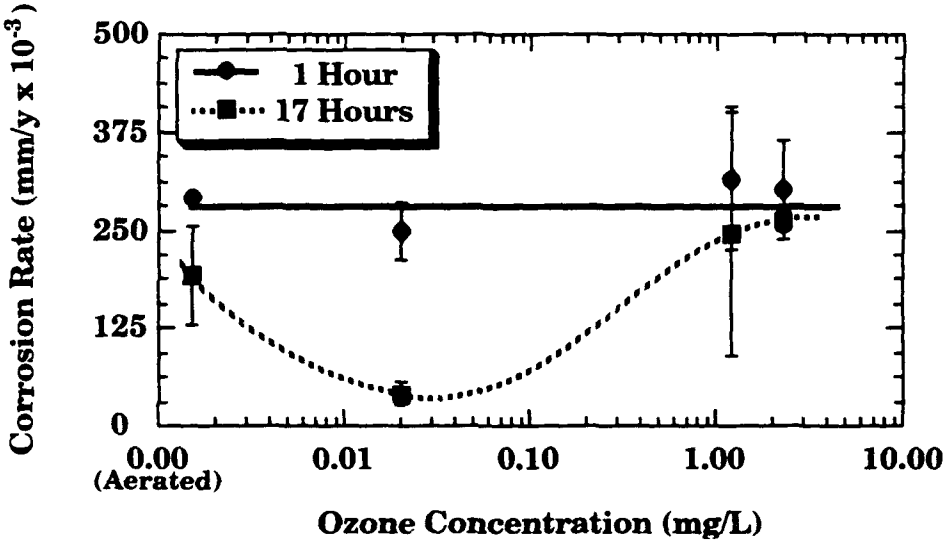

Figure 4.15 The corrosion rate determined from the initial LPR slope of naval brass, as a function of ozone concentration in artificial sea water at 23°C, pH 7.5. This data is believed to reflect the corrosion rate of zinc, which controls the corrosion rate of naval brass in sea water.

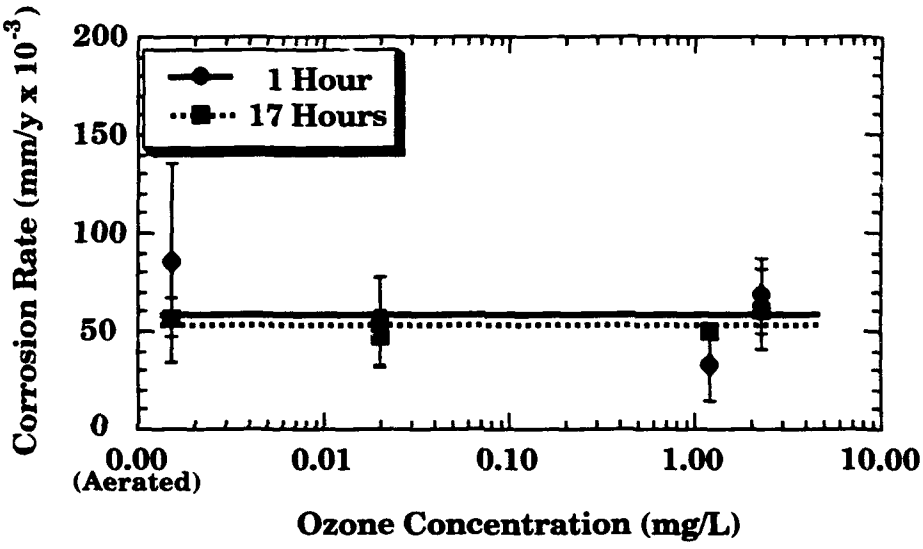

Figure 4.16 The corrosion rate determined from the secondary LPR slope of naval brass, as a function of ozone concentration in artificial sea water at 23°C, pH 7.5. This data is believed to reflect the corrosion rate of copper due to dezincification occurring on the surface.

5. CONCLUSIONS

1. The steady state corrosion potentials of 304 stainless steel and Monel 400 became increasingly noble with increasing ozone concentration due to the noble redox potential of ozone. Extended exposure shifted these values even more noble in the case of stainless steel, indicating that ozone has a large stabilization effect on the passive film compared to oxygen.

2. The corrosion potential of naval brass after one hour was unaffected by the presence of ozone due to the formation of a corrosion product, believed to be a copper oxide. After 17 hours of exposure, all conditions except 2.3 mg/L ozone showed a noble shift in potential which was accompanied by a tarnished brown corrosion product at the surface, believed to be due to dezincification. A gold colored corrosion product was produced on the surface of samples exposed to 2.3 mg/L ozone and is believed to be the same oxide which was formed for all conditions after one hour of exposure.

3. Elevated ozone concentrations shifted the repassivation potential of stainless steel active to the steady state corrosion potential, independent of exposure time. Elevated ozone concentrations also caused the breakdown potential of stainless steel to shift in the active direction relative to the aerated condition after one hour, with extended exposure reversing this effect. These results indicate that stainless steel

has an increased susceptibility to crevice corrosion, especially upon initial exposure to ozone. This effect is believed to be due the presence of either ruptures or defects in the passive film, which decreases as the passive film thickens with time.

4. Elevated ozone concentrations shifted the breakdown and repassivation potential of Monel below the steady state corrosion potential, indicating that this alloy will actively undergo crevice corrosion for these conditions. Extended exposure, however, showed the repassivation potential shifting noble to the steady state corrosion potential, indicating that although pits may still nucleate, they are likely to repassivate before becoming very large.

5. The presence of ozone was found to enhance crevice corrosion in the case of stainless steel, producing slightly more pits than the aerated case with the same median pit area, as well as a few very large deep pits. The formation of these large pits supports the theory of a large cathode/small anode effect existing between the highly stabilized passive film, which formed in the presence of ozone, and the unprotected pits. Crevice corrosion testing of naval brass showed that it was not susceptible to crevice corrosion in either aerated or ozonated solutions.

6. When polarized anodically during LPR testing, naval brass exhibited two distinct slopes. The initial slope was found to represent the corrosion rate of zinc, while the other was found to represent the corrosion

rate of copper, indicating that the process of dezincification was occurring at the metal surface. These corrosion rates were found to be independent of ozone concentration. The exception to this was the case of 0.02 mg/L ozone after 17 hours for which both slopes exhibited values in the range of the corrosion rate of copper, indicating that complete dezincification had occurred on the surface of this alloy before LPR testing. This result shows that low ozone concentrations might actually enhance the process of dezincification with time.

7. For short term exposures, increasing ozone concentrations decreased the corrosion rate of stainless steel compared to the aerated condition due to ozone stabilizing the passive film more rapidly than oxygen. The presence of ozone did not affect the corrosion rate of stainless steel after extended exposure because oxygen stabilized the passive film with time as strongly as observed with ozone. In the case of Monel 400, increasing ozone concentrations caused the corrosion rate to increase, independent of exposure time. This result, coupled with the increase in crevice corrosion susceptibility, show that elevated ozone concentrations are detrimental to this alloy.

6. REFERENCES

1. Ozone in Water and Waste Water Treatment, Editor: F. L. Evans, Ann Arbor Science Publishers Inc., Ann Arbor, MI, p. 83.

2. A.J. Bard, L.R. Faulkner, Electrochemical Methods: Fundamentals and Applications (New York, NY: John Wiley & Sons, 1980) p. 700.

3. S. Hettiarachchi, "The Effects of Ozone on Corrosion of Steel and Copper in Cooling Water Systems," Corrosion/91, 1991, #206.

4. R.P. Rice, J.F. Wilkes, "Fundamental Aspects of Ozone Chemistry in Recirculating Cooling Water Systems," Corrosion/91, 1991, #205.

5. A.G. Hill, R.G. Rice, Handbook of Ozone Technology and Applications (Ann Arbor, MI: Ann Arbor Science Publishers, Inc., 1982) pp. 1-37.

6. K. Kaur, T.R. Bott, B.S.C Leadbeater, Ozone in Water Quality Management (Burgess Hill, Sussex, England: Intl. Ozone Assoc., British Secretariat, 1988) pp. 147-150.

7. H.B. Edwards, *J. Cooling Tower Institute*, 8 (1987): p. 10.

8. D.A. Meier, J.D. Lammering, "A Comparative Use of Ozone Versus Other Chemical Treatments of Cooling Water Systems," *ASHRAE Transactions*, Vol. 93 (Part 2), 1987, pp. 1381-1393.

9. T.S. Lawson, A.E. Feltzin, "Ozonation in a Carbon Dioxide Plant Cooling System," Corrosion/92, 1992, #393.

10. R.J. Strittmatter, B. Yang, D.A. Johnson, "Application of Ozone in Cooling Water Systems," Corrosion/92, 1992, #347.

11. B. Yang, D.A. Johnson, S. H. Shim, "Effect of Ozone on Corrosion of Metals Used in Cooling Towers," *Corrosion*, 49 (1993): p. 499.

12. T.L. Bird, "Corrosion of Mild Steel in Ozonated Air-Conditioning Cooling Tower Water," Electricity Council Research Center, Capenhurst, Chester, CH1 6ES, U.K. Report No. ECR-C/M-2181 (1987), 16 pp. Energy Res. Abstrs. 1988, 13 (7), Abstr. No. 149337.

13. S. Hettiarachchi, "The Effects of Ozone on Corrosion of Steel and Copper in Cooling Water Systems," Corrosion/91, 1991, #206.

14. M. Matsudaira, M. Suzuki, Y. Sato, "Dissolved Ozone Effect on Corrosion of M·tals in Water," *Materials Performance*, 29 (1981): p. 55.

15. N. Kaiga, T. Seki, K. Iyasu, "Ozone Treatment in Cooling Water Systems," *Proceedings, 8th Ozone World Congress,* Vol. 2 (Zurich, Switzerland: Intl. Ozone Association), 1987, pp. G1-G11.

16. J.R. Walton, "The Effect of Ozone on the Corrosion Rate of Metals," May 1983, Presented at 6th Ozone World Congress, Washington D.C. (Norwalk, CT: Intl. Ozone Assoc.).

17. H.H. Lu, D.J. Duquette, "The Effect of Dissolved Ozone on the Corrosion Behavior of Cu-30Ni and 304L Stainless Steel in 0.5N NaCl Solutions", *Corrosion,* 46 (1990): p.843.

18. B.E. Brown, H.H. Lu, D.J. Duquette, "Effect of Flow Rates on Localized Corrosion Behavior of 304 Stainless Steel in Ozonated 0.5N NaCl", *Corrosion*, 48 (1992): p.970.

19. A. Kyas, R. Wellauer, M. Oldani, "Cooling Water Treatment with Ozone," 1989, in *Ozone in Wastewater Treatment & Industrial Applications, Proceedings 9th Ozone World Congress,* Vol. 2, L.J. Bollyky, Editor (Norwalk, CT: Intl. Ozone Assoc., 1989), pp. 300-306.

20. R. Wellauer, M. Oldani, "Cooling Water Treatment with Ozone," *Ozone Science and Engineering*, 12(1990): p. 243.

21. J. W. Oldfield, B. Todd, *Desalination*, 38 (1981): p. 233.

22. M. Stern, A. Geary, *J. Electrochem. Soc.*, 56 (1957): p. 104.

23. H.H. Uhlig, R.W. Revie, Corrosion and Corrosion Control (New York, NY: John Wiley & Sons, 1985), p. 71.

23. H.H. Uhlig, Corrosion Handbook (New York, NY: John Wiley & Sons, 1948), p. 397.

7. APPENDIX

The Effect of Assumed Tafel Values on Corrosion Rates Calculated from Linear Polarization Resistance Measurements:

$$R_p = \frac{dE}{dI}$$

$$i_{CORR} = \left(\frac{1}{2.3 \times R_p \times AREA}\right)\left(\frac{\beta_a \times \beta_c}{\beta_a + \beta_c}\right)$$

If $\beta_a = \beta_c = 0.05$:

$$i_{CORR} = \frac{\mathbf{0.0109}}{\mathbf{R_p \times AREA}}$$

If Concentration Polarization Occurs:

$$i_{CORR} = \left(\frac{\beta_a}{2.3 \times R_p \times AREA}\right)$$

If $\beta_a = 0.12$:

$$i_{CORR} = \frac{\mathbf{0.0522}}{\mathbf{R_p \times AREA}}$$

Difference between assuming $\beta_a = \beta_c = 0.05$ and assuming that concentration polarization occurs with $\beta_a = 0.12$:

$$\textbf{Difference} = \frac{\mathbf{0.0522}}{\mathbf{0.01087}} = \mathbf{4.8}$$

Determination of Corrosion Rates from Linear Polarization Resistance Measurements:

$$R_p = \frac{dE}{dI}$$

$$i_{CORR} = \left(\frac{1}{2.3 \times R_p \times AREA}\right)\left(\frac{b_a \times b_c}{b_a + b_c}\right)$$

If $\beta_a = \beta_c = 0.12$:

$$\mathbf{i_{CORR} = \frac{0.0261}{R_p \times AREA}}$$

$$\frac{mm}{y} = 1.734\,(i_{CORR})$$

$$\frac{mm}{y} = 1.734\left(\frac{0.0261}{R_p \times AREA}\right)$$

$$\mathbf{\frac{mm}{y} = \frac{0.0453}{R_p \times AREA}}$$

If $\beta_a = \beta_c = 0.05$:

$$\mathbf{i_{CORR} = \frac{0.01087}{R_p \times AREA}}$$

$$\frac{mm}{y} = 1.734\,(i_{CORR})$$

$$\frac{mm}{y} = 1.734\left(\frac{0.01087}{R_p \times AREA}\right)$$

$$\mathbf{\frac{mm}{y} = \frac{0.0188}{R_p \times AREA}}$$

Calculation of the Anodic Curve of Stainless Steel :

Concentration Polarization Assumed

$$i_L = \frac{DnFC}{\delta t} \times 10^{-3}$$

$t = 1$ $\qquad C = \frac{moles}{L}$

$\delta = 0.05$ cm $\qquad D = 5 \times 10^{-5} \frac{cm^2}{s}$

$n = 2$

$$i_L = 0.1nC$$

For 1.2 mg/L

$$C = \left(1.2 \times 10^{-3} \frac{g}{L} \right)\left(\frac{1 \text{ mole}}{48 \text{ g}}\right) = 2.5 \times 10^{-5} \frac{moles}{L}$$

$n = 2$

$$i_L = 0.1(2)(2.5 \times 10^{-5})$$

$$i_L = 5 \times 10^{-6} \frac{A}{cm^2}$$

For 2.3 mg/L

$$C = \left(2.3 \times 10^{-3} \frac{g}{L} \right)\left(\frac{1 \text{ mole}}{48 \text{ g}}\right) = 4.8 \times 10^{-5} \frac{moles}{L}$$

$n = 2$

$$i_L = 0.1(2)(4.8 \times 10^{-5})$$

$$i_L = 1 \times 10^{-5} \frac{A}{cm^2}$$

For Air Saturation:

$$C = \left(7.85 \times 10^{-3} \frac{g}{L} \right)\left(\frac{1 \text{ mole}}{32 \text{ g}}\right) = 2.4 \times 10^{-4} \frac{\text{moles}}{L}$$

$n = 2$

$$i_L = 0.1(2)(2.4 \times 10^{-4})$$

$$i_L = 4.9 \times 10^{-5} \frac{A}{cm^2}$$

Reversible Potential of Oxygen:

$$O_2 + 4H^+ + 4e^- \rightarrow 2\ H_2O$$

$$E = E_0 - \frac{0.059}{n} \log\left(\frac{1}{pO_2}\right)$$

$n = 4$
$E_0 = 1.229$ V vs.. SHE

Find pO_2:

From Uhlig - Aerated solutions contain 7.85 mg/L of oxygen

$$pO_2 = \frac{\left(7.85 \times 10^{-3} \frac{g}{L}\right)\left(\frac{1 \text{ mole}}{32 \text{ g}}\right)(0.0821)\,(298)}{1L}$$

$pO_2 = 6 \times 10^{-3}$ atm

$$E = 1.229 - \frac{0.059}{4} \log\left(\frac{1}{6 \times 10^{-3}}\right)$$

$E = 1.229 - 0.033$

$E = 1.20$ V vs.. SHE

$E = 0.96$ V vs.. SCE

Reversible Potential of Ozone:

$$O_3 + 6H^+ + 6e^- \rightarrow 3\ H_2O$$

$$E = E_0 - \frac{0.059}{n} \log\left(\frac{aH_20}{aO_3}\right)$$

n = 6
E_0 = 2.07 V vs. SHE
aH_20 = 1

Find aO_3:

For 1.2 mg/L

$$aO_3 = \frac{\left(1.2 \times 10^{-3}\ \frac{g}{L}\right)\left(\frac{1\ mole}{48\ g}\right)(0.0821)\ (298)}{1L}$$

$pO_3 = 6.1 \times 10^{-4}$ atm

$$E = 2.07 - \frac{0.059}{6} \log\left(\frac{1}{6 \times 10^{-4}}\right)$$

E = 2.07 - 0.032
E = 2.04 V vs.. SHE
E = 1.80 V vs.. SCE

For 2.3 mg/L

$$aO_3 = \frac{\left(2.3 \times 10^{-3}\ \frac{g}{l}\right)\left(\frac{1\ mole}{48\ g}\right)(0.0821)\ (298)}{1L}$$

$pO_3 = 1.3 \times 10^{-3}$ atm

$$E = 2.07 - \frac{0.059}{6} \log\left(\frac{1}{1.2 \times 10^{-3}}\right)$$

E = 2.07 - 0.029
E = 2.04 V vs.. SHE
E = 1.77 V vs.. SCE

Find i_C in terms of i_L and dE:

$$\Delta E = \frac{-RT}{nF} \ln\left(\frac{i_L}{i_L - i_C}\right)$$

$$\exp\left(\frac{-\Delta EnF}{RT}\right) = \frac{i_L}{i_L - i_C}$$

$$i_L = (i_L - i_C)\left(\exp\left(\frac{-\Delta EnF}{RT}\right)\right)$$

$$i_C = i_L - \frac{i_L}{\exp\left(\frac{\Delta EnF}{RT}\right)}$$

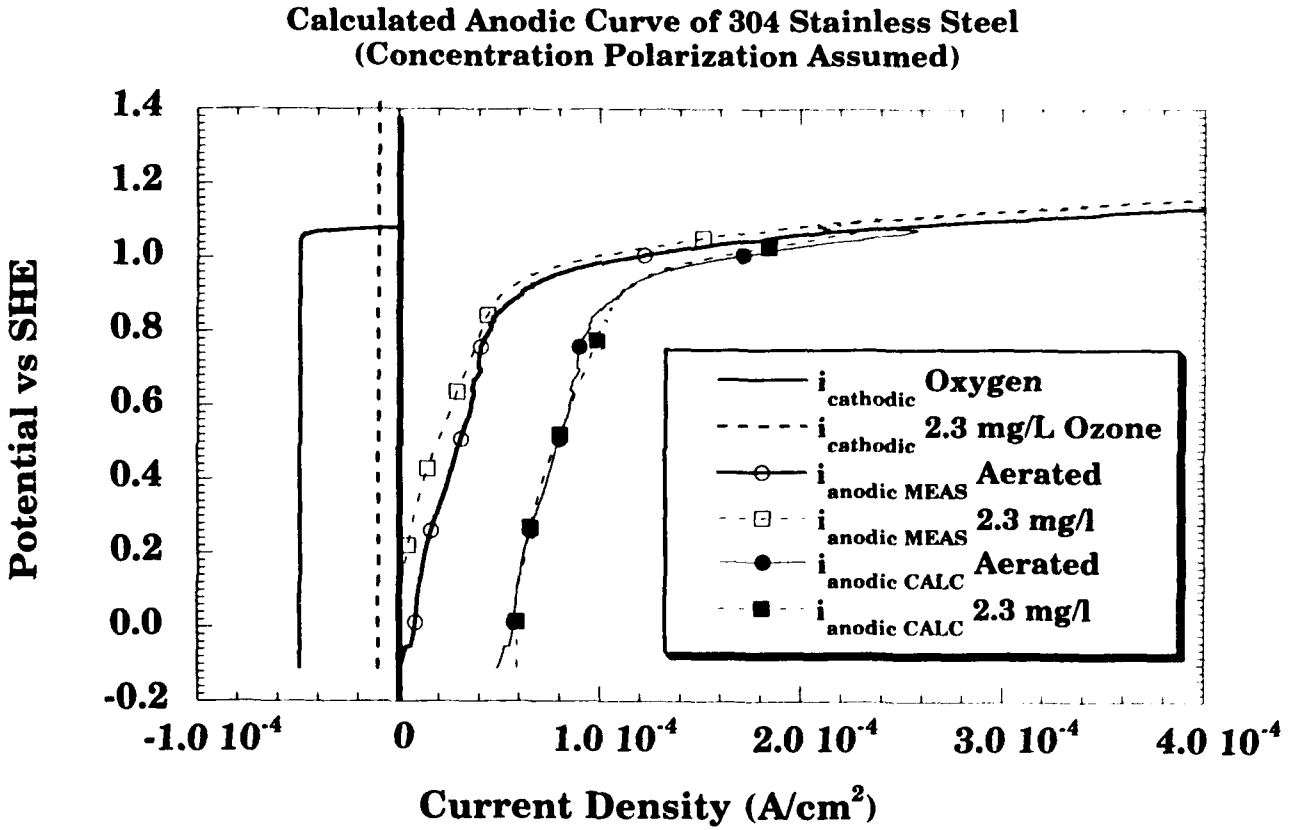
Calculated Anodic Curve of 304 Stainless Steel
(Concentration Polarization Assumed)
Potential vs SHE
1.4
1.2
1.0
0.8
0.6
0.4
0.2
0.0
-0.2
-1.0 10-4
0
1.0 10-4
2.0 10-4
3.0 10-4
4.0 10-4
Current Density (A/cm2)
icathodic Oxygen
icathodic 2.3 mg/L Ozone
ianodic MEAS Aerated
ianodic MEAS 2.3 mg/l
ianodic CALC Aerated
ianodic CALC 2.3 mg/l

Cyclic Polarization Curves of 304 Stainless Steel Wire After 1 Hour Exposure to Artificial Sea Water, pH 7.5, 23°C

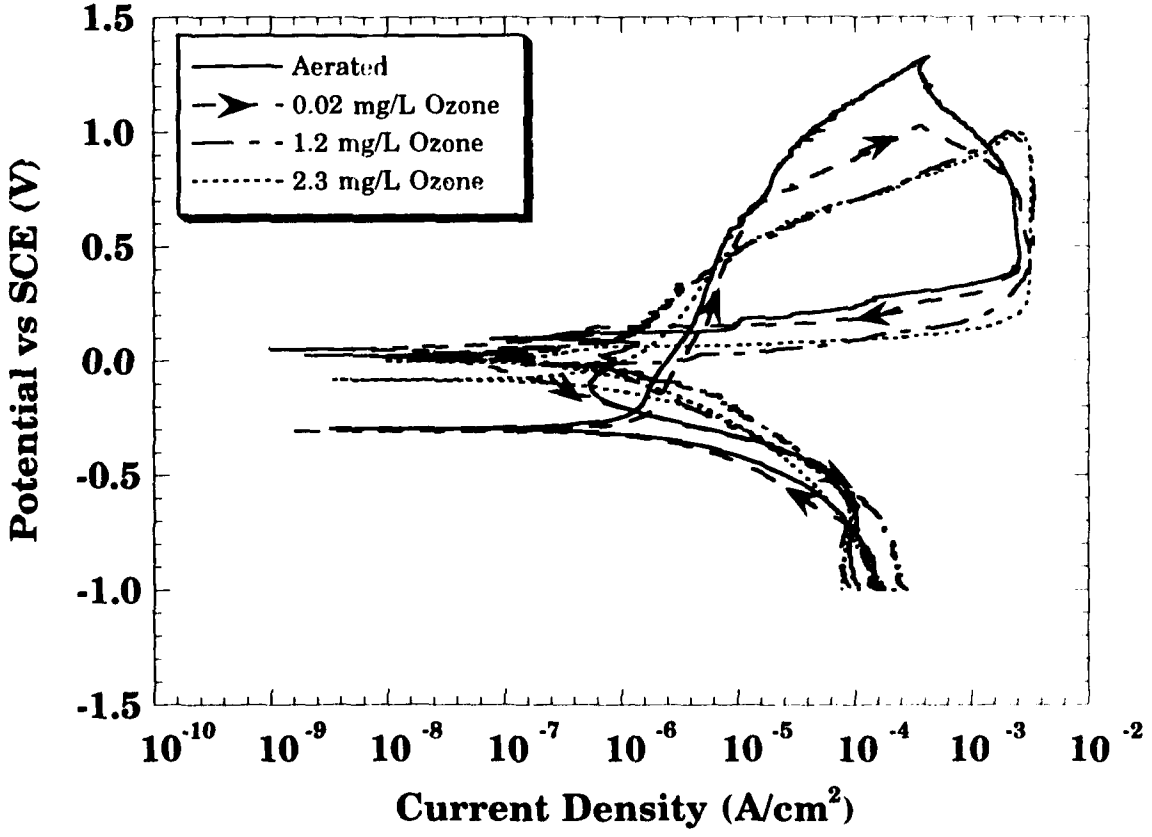

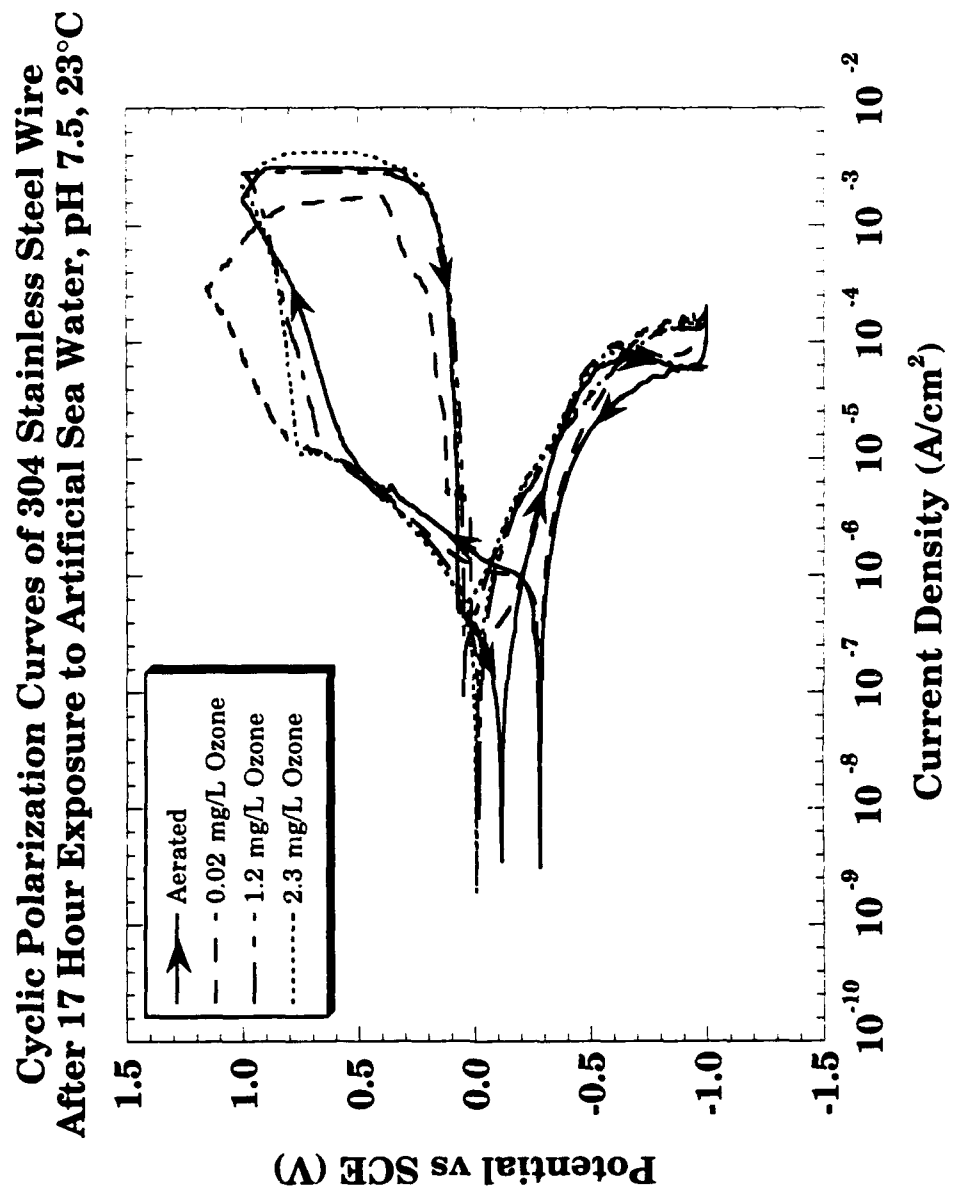
Cyclic Polarization Curves of 304 Stainless Steel Wire
After 17 Hour Exposure to Artificial Sea Water, pH 7.5, 23°C
Aerated
0.02 mg/L Ozone
1.2 mg/L Ozone
2.3 mg/L Ozone
Potential vs SCE (V)
1.5
1.0
0.5
0.0
-0.5
-1.0
-1.5
Current Density (A/cm²)
10⁻¹⁰
10⁻⁹
10⁻⁸
10⁻⁷
10⁻⁶
10⁻⁵
10⁻⁴
10⁻³
10⁻²

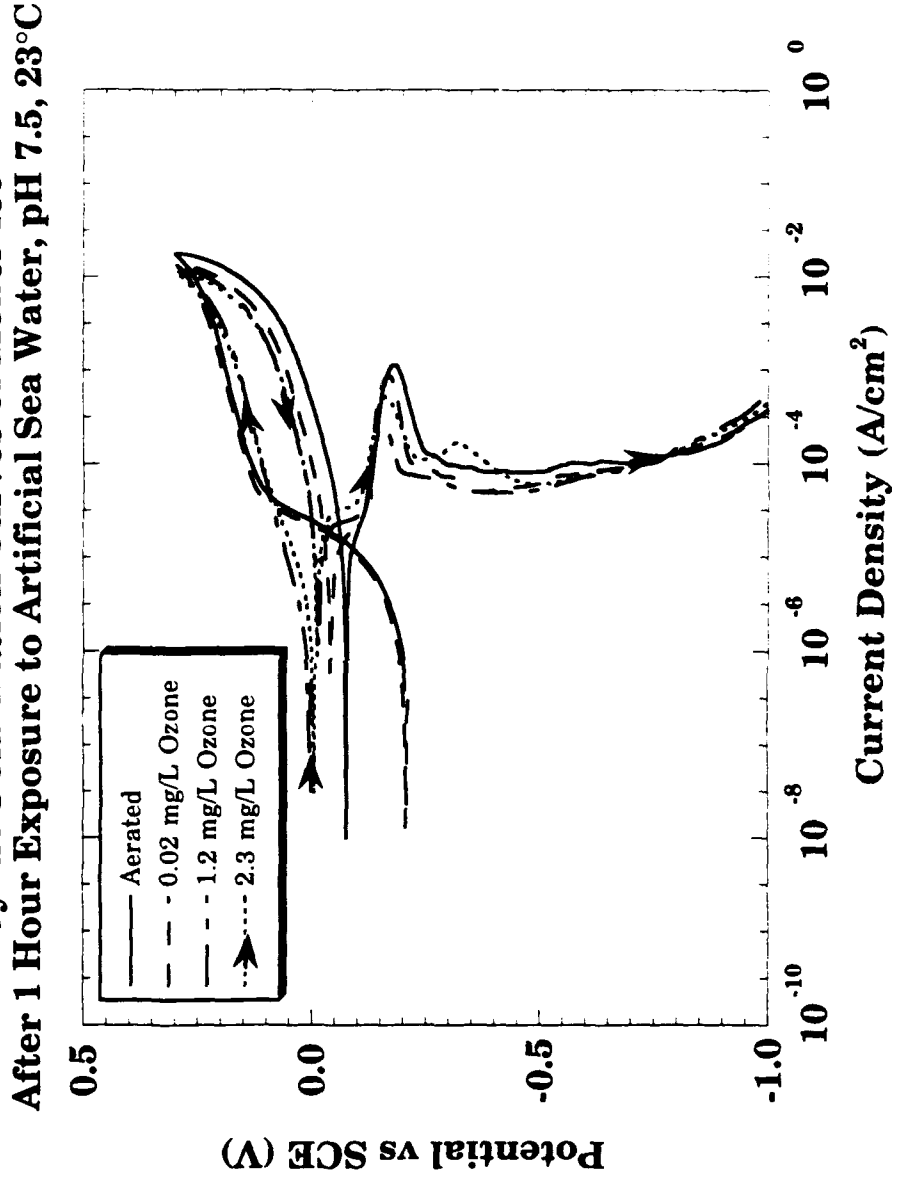
Cyclic Polarization Curves of Monel 400
After 1 Hour Exposure to Artificial Sea Water, pH 7.5, 23°C
Aerated
0.02 mg/L Ozone
1.2 mg/L Ozone
2.3 mg/L Ozone
Potential vs SCE (V)
0.5
0.0
-0.5
-1.0
Current Density (A/cm²)
10⁻¹⁰
10⁻⁸
10⁻⁶
10⁻⁴
10⁻²
10⁰

Cyclic Polarization Curves of Monel 400
After 17 Hour Exposure to Artificial Sea Water, pH 7.5, 23°C

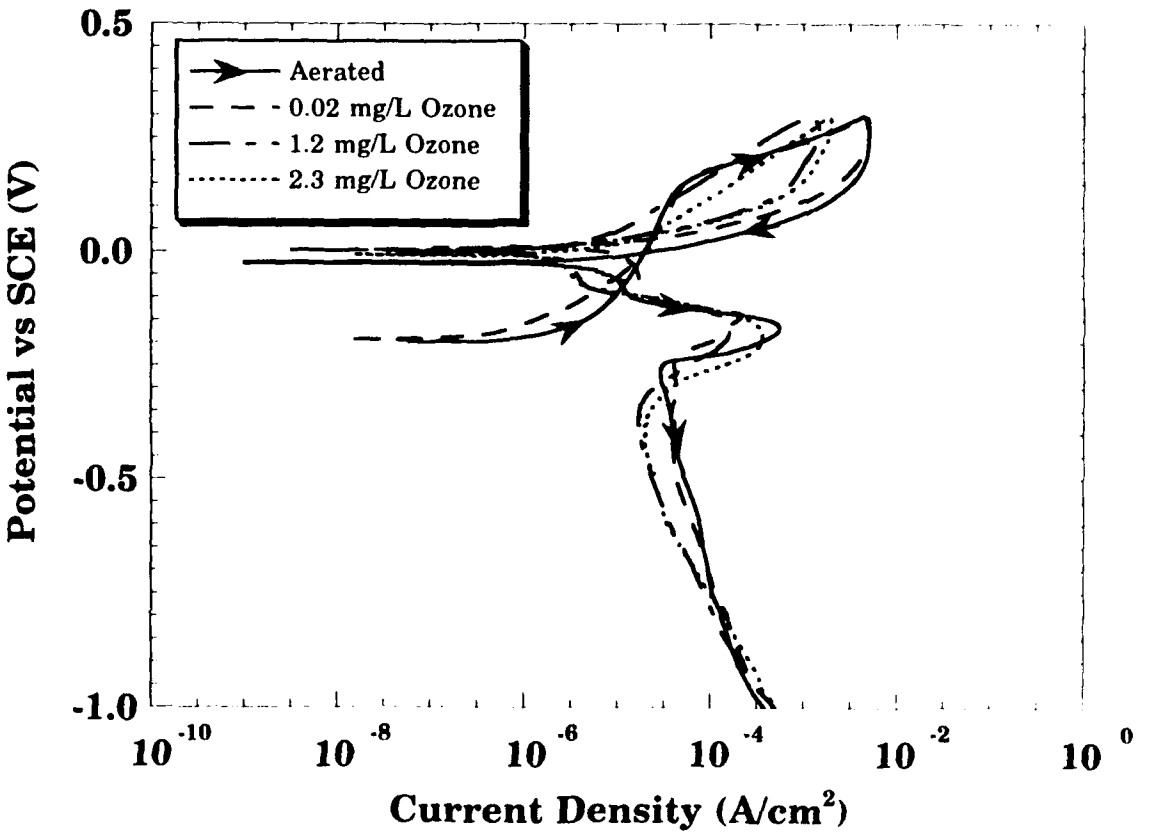

304 SS WIRE
1 hour, Aerated

Ecorr	mm/yr x 10^{-3}	Ezero	Ep (mV)	Eb (mV)	Eb-Ep	Ep-Ecorr	Ep-Ezero
-202	1.06	-328	144	536	392	346	472
-190	1.36	-314	64	616	552	254	378
-204	1.30	-294	130	534	424	334	424
-199±8	1.24±0.16	-312±17	113±43	569±42	456±85	311±50	425±47

304 SS WIRE
17 hours, Aerated

Ecorr	mm/yr x 10^{-3}	Ezero	Ep (mV)	Eb (mV)	Eb-Ep	Ep-Ecorr	Ep-Ezero
-59	0.26	-276	50	668	422	109	326
-44	0.45	-290	246	546	468	290	536
-60	0.38	-282	78	426	376	138	360
-54±9	0.37±0.09	-283±7	125±106	547±121	422±26	179±97	407±13

304 SS WIRE
1 hour, 0.02 mg/L

Ecorr	mm/yr x 10^{-3}	Ezero	Ep (mV)	Eb (mV)	Eb-Ep	Ep-Ecorr	Ep-Ezero
-198	1.34	-306	130	532	402	328	436
-207	1.58	-314	96	628	532	303	410
-189	1.07	-306	156	690	534	345	462
-198±9	1.33±0.26	-309±5	127±30	617±80	489±76	325±21	436±26

304 SS WIRE
17 hours, 0.02 mg/L

Ecorr	mm/yr x 10^{-3}	Ezero	Ep (mV)	Eb (mV)	Eb-Ep	Ep-Ecorr	Ep-Ezero
81	0.21	-248	14	548	534	-67	262
-50	0.89	-274	116	576	460	166	390
94	0.25	-270	104	642	538	10	374
42±80	0.45±0.38	-264±14	78±56	589±48	511±44	36±119	342±70

304 SS WIRE
1 hour, 1.2 mg/L

Ecorr	mm/yr x 10^{-3}	Ezero	Ep (mV)	Eb (mV)	Eb-Ep	Ep-Ecorr	Ep-Ezero
72	0.88	-88	152	486	334	80	240
97	0.93	-52	212	478	266	115	264
50	1.16	-180	28	498	470	-22	208
73±24	0.99±0.15	-107±66	131±94	487±10	357±104	58±71	237±28

304 SS WIRE
17 hours, 1.2 mg/L

Ecorr	mm/yr x 10^{-3}	Ezero	Ep (mV)	Eb (mV)	Eb-Ep	Ep-Ecorr	Ep-Ezero
159	0.23	-14	76	538	462	-83	90
92	0.43	12	110	570	460	18	98
89	0.50	-20	48	648	600	-41	68
113±40	0.39±0.14	-7±17	78±31	585±57	507±80	-35±51	85±16

304 SS WIRE
1 hours, 2.3 mg/L

Ecorr	mm/yr x 10^{-3}	Ezero	Ep (mV)	Eb (mV)	Eb-Ep	Ep-Ecorr	Ep-Ezero
74	1.08	-84	62	456	394	-12	146
114	0.66	-34	22	502	480	-92	56
74	1.01	-38	8	486	478	-66	46
87±23	0.92±0.23	-52±28	31±28	481±23	451±49	-57±41	86±55

304 SS WIRE
17 hours, 2.3 mg/L

Ecorr	mm/yr x 10^{-3}	Ezero	Ep (mV)	Eb (mV)	Eb-Ep	Ep-Ecorr	Ep-Ezero
240	0.28	-10	80	706	626	-160	90
258	0.25	-14	62	684	622	-196	76
234	0.33	8	50	746	696	-184	58
244±12	0.29±0.04	-11±3	64±15	712±31	648±42	-180±18	75±16

Monel 400
1 hour, Aerated

Ecorr	mm/yr x 10^{-3}	Ep (mV)	Eb (mV)	Eb-Ep	Ep-Ecorr	Ep-Ezero
-208	33	-72	88	160	136	-72
-206	19	-62	106	168	144	-62
-210	21	-30	130	160	180	-30
-208±2	24±7	-55±22	108±21	163±5	153±23	-55±22

Monel 400
17 hours, Aerated

Ecorr	mm/yr x 10^{-3}	Ep (mV)	Eb (mV)	Eb-Ep	Ep-Ecorr	Ep-Ezero
-204	10	-5	143	148	193	-5
-198	15	-21	119	140	9	-21
-204	22	20	164	144	224	20
-202±3	15±6	-2±21	142±23	144±4	142±116	-22±1

Monel 400
1 hour, 0.02 mg/L

Ecorr	mm/yr x 10^{-3}	Ep (mV)	Eb (mV)	Eb-Ep	Ep-Ecorr	Ep-Ezero
-212	19	14	120	136	195	-19
-211	15	0	112	112	211	0
-206	20	-30	104	134	176	-30
-210±3	18.1±2.5	-16±12	111±5	127±11	194±14	-16±12

Monel 400
17 hours, 0.02 mg/L

Ecorr	mm/yr x 10^{-3}	Ep (mV)	Eb (mV)	Eb-Ep	Ep-Ecorr	Ep-Ezero
-143	2.0	26	130	104	237	26
-211	2.7	31	155	124	231	31
-200	2.8	10	138	128	74	10
-185±37	2.5±0.5	19±11	151±22	106±64	168±68	15±13

Monel 400
1 hour, 1.2 mg/L

Ecorr	mm/yr x 10^{-3}	Ep (mV)	Eb (mV)	Eb-Ep	Ep-Ecorr	Ep-Ezero
-6	31	-27	93	130	-28	-34
-2	16	-34	96	94	12	10
0	34	-14	110	124	-14	-14
-3±3	27.0±9.3	-25±10	100±9	125±5	-9±22	-25±10

Monel 400
17 hours, 1.2 mg/L

Ecorr	mm/yr x 10^{-3}	Ep (mV)	Eb (mV)	Eb-Ep	Ep-Ecorr	Ep-Ezero
-14	45	12	180	168	68	12
-26	11	15	177	162	29	15
-8	22	18	210	192	44	18
-16±9	25.8±17.4	15±3	189±18	174±16	47±20	15±3

Monel 400
1 hours, 2.3 mg/L

Ecorr	mm/yr x 10^{-3}	Ep (mV)	Eb (mV)	Eb-Ep	Ep-Ecorr	Ep-Ezero
1	110	-19	95	114	-21	-19
2	69	-11	100	111	-12	-11
-14	61	-19	147	166	-5	-19
-4±9	80±26	-16±5	114±29	130±31	-13±8	-16±5

Monel 400
17 hours, 2.3 mg/L

Ecorr	mm/yr x 10^{-3}	Ep (mV)	Eb (mV)	Eb-Ep	Ep-Ecorr	Ep-Ezero
-17	85	28	200	100	23	13
-10	62	13	224	165	52	35
-20	80	35	162	126	35	36
-15±4	76±12	25±11	158±44	130±33	37±15	28±13

Naval Brass
1 hour, Aerated

Ecorr	ZINC mm/y x 10^{-3}	COPPER mm/y x 10^{-3}
-263	286	62.3
-263	293	48.7
-269	296	143
-265±3	292±5	85±51

Naval Brass
17 hours, Aerated

Ecorr	ZINC mm/y x 10^{-3}	COPPER mm/y x 10^{-3}
-241	154	66
-221	266	28
-233	156	31
-246±4	192±64	41±21

Naval Brass
1 hour, 0.02 mg/L

Ecorr	ZINC mm/y x 10^{-3}	COPPER mm/y x 10^{-3}
-265	226	81
-262	228	37
-264	289	47
-264±2	248±36	55±23

Naval Brass
17 hours, 0.02 mg/L

Ecorr	ZINC mm/y x 10^{-3}	COPPER mm/y x 10^{-3}
-235	46	17
-238	52	9
-236	26	13
-236±2	41±14	13±4

Naval Brass
1 hour, 1.2 mg/L

Ecorr	ZINC mm/y x 10^{-3}	COPPER mm/y x 10^{-3}
-257	309	30
-261	408	16
-274	226	54
-264±9	315±91	33±19

Naval Brass
17 hours, 1.2 mg/L

Ecorr	ZINC mm/y x 10^{-3}	COPPER mm/y x 10^{-3}
-252	415	50
-236	202	29
-235	113	45
-244±10	246±155	41±11

Naval Brass
1 hours, 2.3 mg/L

Ecorr	ZINC mm/y x 10^{-3}	COPPER mm/y x 10^{-3}
-274	374	86
-278	271	47
-279	260	71
-277±3	302±63	68±19

Naval Brass
17 hours, 2.3 mg/L

Ecorr	ZINC mm/y x 10^{-3}	COPPER mm/y x 10^{-3}
-260	274	83
-268	262	57
-259	247	43
-262±5	261±14	61±20

Unclassified
SECURITY CLASSIFICATION OF THIS PAGE

REPORT DOCUMENTATION PAGE

Form Approved
OMB No. 0704-0188

1a. REPORT SECURITY CLASSIFICATION Unrestricted	1b. RESTRICTIVE MARKINGS None
2a. SECURITY CLASSIFICATION AUTHORITY	3. DISTRIBUTION/AVAILABILITY OF REPORT Unrestricted
2b. DECLASSIFICATION/DOWNGRADING SCHEDULE	
4. PERFORMING ORGANIZATION REPORT NUMBER(S)	5. MONITORING ORGANIZATION REPORT NUMBER(S)
6a. NAME OF PERFORMING ORGANIZATION Rensselaer Polytechnic Institute 6b. OFFICE SYMBOL (If applicable)	7a. NAME OF MONITORING ORGANIZATION
6c. ADDRESS (City, State, and ZIP Code) Troy, NY 12180-3590	7b. ADDRESS (City, State, and ZIP Code)
8a. NAME OF FUNDING/SPONSORING ORGANIZATION Office of Naval Research 8b. OFFICE SYMBOL (If applicable)	9. PROCUREMENT INSTRUMENT IDENTIFICATION NUMBER
8c. ADDRESS (City, State, and ZIP Code) 800 N. Quincy Street Arlington, VA 22217-5000	10. SOURCE OF FUNDING NUMBERS PROGRAM ELEMENT NO. / PROJECT NO. / TASK NO / WORK UNIT ACCESSION NO

11. TITLE (Include Security Classification)
The Effects of Dissolved Ozone on the Corrosion Behavior of 304 Stainless Steel, Monel 400 and Naval Brass in Artificial Sea Water

12. PERSONAL AUTHOR(S)
B.E. Brown and D.J. Duquette

13a. TYPE OF REPORT	13b. TIME COVERED	14. DATE OF REPORT (Year, Month, Day)	15. PAGE COUNT
Final	FROM 1/90-10/93	November 1, 1993	75

16. SUPPLEMENTARY NOTATION
NONE

17. COSATI CODES			18. SUBJECT TERMS (Continue on reverse if necessary and identify by block number)
FIELD	GROUP	SUB-GROUP	Corrosion, Stainless Steel, Copper Nickel Alloy, Dissolved Ozone, Chloride Solutions

19. ABSTRACT (Continue on reverse if necessary and identify by block number)

The effects of 0.02, 1.2 and 2.3 mg/L ozone on the corrosion behavior of 304 stainless steel, Monel 400, and naval brass were studied at room temperature in artificial sea water at pH 7.5, and the results were compared with those obtained for aerated solutions. Corrosion potentials and cyclic polarization curves were measured after 1 and 17 hour expsoure times. Instantaneous corrosion rates were measured using linear polarization resistance (LPR) techniques. Long term (30 day) crevice corrosion experiments were also performed on stainless steel and naval brass in aerated and 0.8 mg/L ozonated solutions.

Increasingly noble corrosion potentials were observed in the cases of stainless steel and Monel with increasing ozone concentration due to the noble redox potential of ozone. Nava brass, on the other hand, maintained a fairly constant corrosion potential, independent of ozone concentration, due to the formation of a bulk corrosion product on the metal surface.

LPR measurements on naval brass reflected the corrosion rates of both zinc and copper due to dezincification occurring on the metal surface. These corrosion rates were found to

20. DISTRIBUTION/AVAILABILITY OF ABSTRACT ☒ UNCLASSIFIED/UNLIMITED ☐ SAME AS RPT. ☐ DTIC USERS	21. ABSTRACT SECURITY CLASSIFICATION Unrestricted
22a. NAME OF RESPONSIBLE INDIVIDUAL D.J. Duquette	22b. TELEPHONE (Include Area Code) 518-276-6459 22c. OFFICE SYMBOL

DD Form 1473, JUN 86 *Previous editions are obsolete.* SECURITY CLASSIFICATION OF THIS PAGE